THE ALASKA COASTAL CURRENT:

AN ANALYTICAL APPROACH

RECOMMENDED:

Henry J. Niebauer

Robert T. Cooney

Thomas C. Royer
Chairman, Advisory Committee

[signature]
Director, Division of Marine Sciences

APPROVED:

W. S. Reeburgh
Director of Graduate Programs

13 December 1983
Date

THE ALASKA COASTAL CURRENT:

AN ANALYTICAL APPROACH

A

THESIS

Presented to the Faculty of the

University of Alaska in partial fulfillment

of the Requirements

for the Degree of

MASTER OF SCIENCE

By

Gregory A. Vayda, B.S.

Fairbanks, Alaska

December 1983

ABSTRACT

THE ALASKA COASTAL CURRENT:

AN ANALYTICAL APPROACH

A steady-state, analytical model has been developed to investigate the dynamic interaction of alongshore wind and coastal fresh water discharge that serve as forcing functions to drive a coastal current. The coastal current, which is considered here, flows westward and borders the southern and southeastern coastal regions of Alaska. Given average monthly values for fresh water discharge of 23000 m^3 s^{-1} for 1300 km of coastline, and an easterly wind of 6 m s^{-1}, the model yields a 35 day transit time for the coastal current. This transit time and a total predicted transport of 1,096,000 m^3 s^{-1}, for the current, are in good agreement with direct observations. The model can be used to predict the response of the coastal current to various wind intensities and fresh water discharges.

TABLE OF CONTENTS

LIST OF FIGURES

LIST OF TABLES

PREFACE

The following pages contain a number of mathematical complexities, assumptions, rationales, and conclusions about a phenomenon of nature. It is of the utmost importance to realize that this thesis in no way purports to reveal any absolute truth about nature. The most that we can hope to achieve is a representation of the observed phenomenon, in this case, mathematical. Here we consider some process which yields the properties, velocity and transport, that are similar to those observed in the actual coastal current. The process we use in modelling may or may not have anything to do with the actual current. By the same token we can consider light emitted from a light bulb. The internal process is thought to be small particles, electrons, transitioning to different levels around the outside of the nucleus, thus producing the light we see. This internal process may or may not occur, but it explains the observations. There is not anything sinister in this process of modelling the observations with processes that may or may not occur. On the pragmatic side of things, we can still make the machines work.

In driving the nail squarely on its head, I feel that the motivations and results of the artist and scientist are very similar, if not related. Both groups wish to describe something. Intuitive thought is a paramount ingredient whether using mathematics or applying paint to canvas. The main difference between the groups are the tools they use to achieve their goals. Whether it consists of mathematical equations, poetry, painting, or music to describe some phenomenon, we are merely representing our observations regardless of the reality of the object observed or the processes involved.

Chapter I   INTRODUCTION

The Alaska Coastal Current is an energetic, narrow band of low density water which flows westward along the northern border of the Gulf of Alaska. The intent of this thesis is to investigate some aspects of the physics of this current. Figure 1 depicts the general flow scheme of the coastal current. High precipitation rates in the coastal mountains that border the northeast Pacific Ocean produce large fresh water discharges which are energy sources for the coastal current. As the low density fresh water enters the ocean it overflows the denser, ambient sea water. Due to rotation effects, the overflow is deflected to the right and then flows along the coast to the west. In addition to this outflow, the alongshore easterly wind acts as another energy source, moving the fresh water shoreward and maintains the fresh water as a narrow band. The fresh water enters the ocean via a number of small rivers and streams; therefore, it is treated as a line source instead of multiple point sources. Inspections of hydrographic data, from cross sections of the Alaska Coastal Current, indicate a relationship between the incoming fresh water, wind, and the resulting flow of the coastal current (Royer, 1982).

There have been several papers in the last few years which have dealt with fresh water driven baroclinic coastal circulation (Griffiths and Linden [1981], Haakstad [1977], Heaps [1972, 1980], Kao [1981], and Pietrafesa and Janowitz [1979]). Fewer publications consider both fresh water and wind forcing of coastal circulation (Csanady [1976], Leetma [1976], and Stommel and Leetma [1972]). Existing models use the equations of motion common to oceanographic analysis. This thesis considers

10
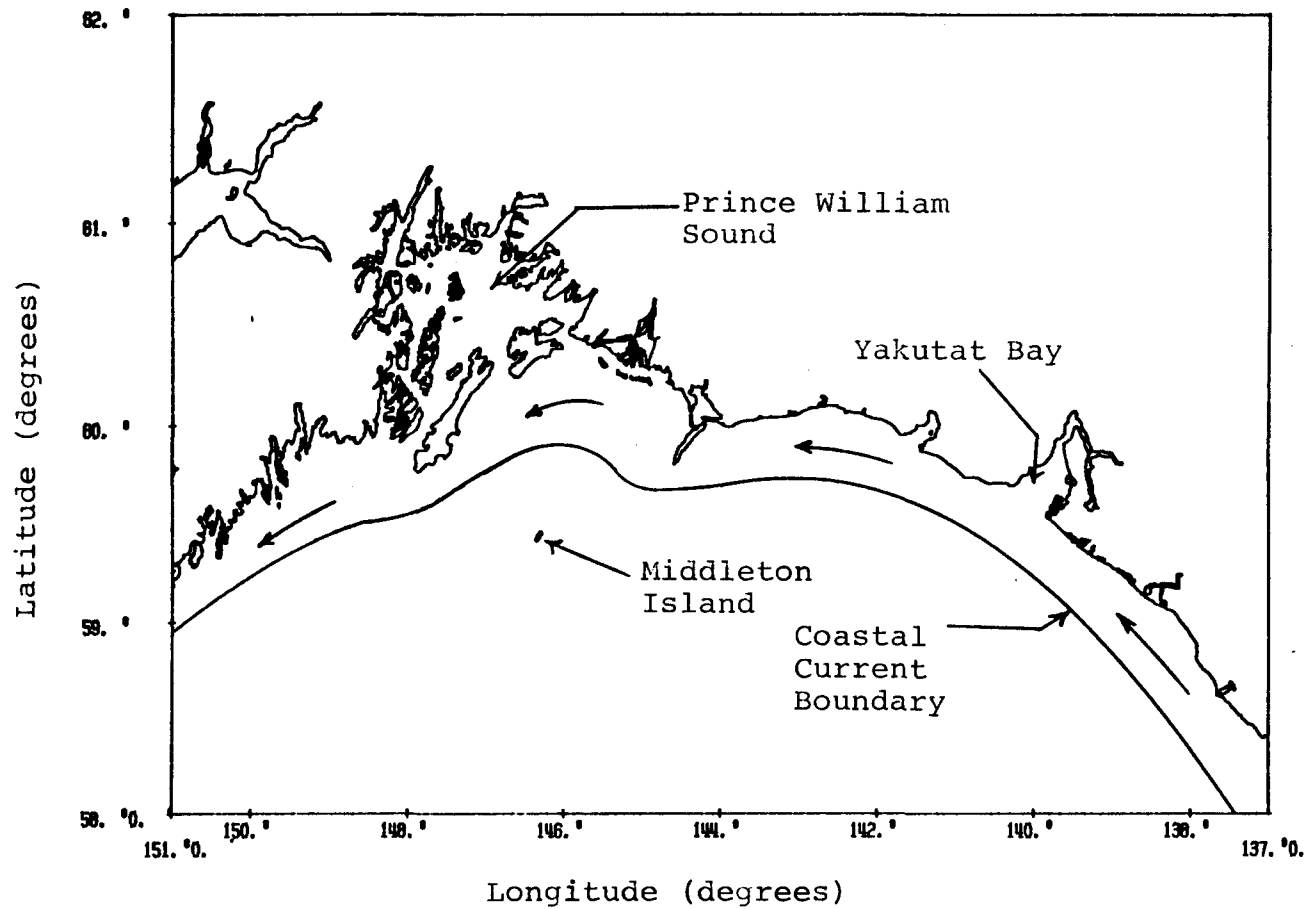
Figure 1 – Geographical setting for the Alaska Coastal Current.

the physical system to be analogous to an electrical capacitor and uses
equations appropriate to this concept. The objective of the analytical
model developed here is to relate the wind and fresh water forcing to
the resultant flow of the Alaska Coastal Current.

Chapter II   MODEL

Figure 2 illustrates an idealized straight coastline with a constant fresh water discharge and steady wind field. Cartesian coordinates x, y, and z form a left-handed set where x and y, respectively, are the cross-shelf and alongshore distances, and z is the depth beneath the surface.

A balance of power is the central tenet of this model. Power is defined as the energy flow per unit time normal to a surface. For a steady-state system, the sum of the power inputs must equal the sum of the power outputs. In our case, the power from wind and fresh water must equal the power of the induced coastal current. The power from the coastal current is an addition to the ambient power from the alongshore flow.

To prevent confusion, the model was formulated in two steps. The first step determined the power as a function of fresh water discharge and the second step determined the power as a function of fresh water discharge and alongshore wind.

The following assumptions outline the framework within which the model was constrained;

1) no mixing between fresh and sea water,

2) the system is in steady-state,

3) fresh water discharge is steady and acts as a line source,

4) alongshore wind field is steady and uniform,

5) the coast is straight and uniform,

6) the Coriolis parameter is a constant,

7) air density and drag coefficient are constant,

8) constant shelf depth, and

9) no horizontal friction.
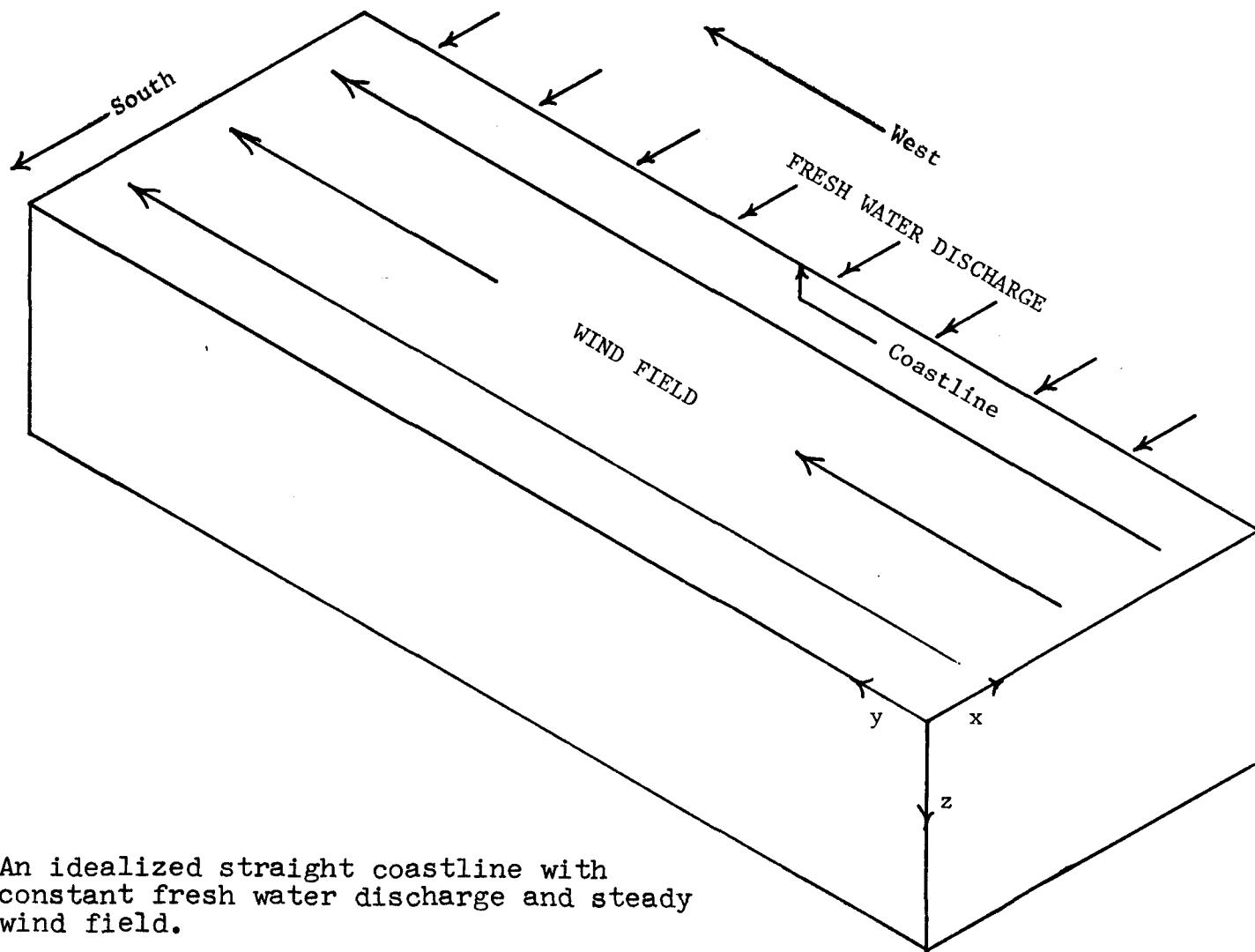
Figure 2 – An idealized straight coastline with
constant fresh water discharge and steady
wind field.

FRESH WATER FORCING WITHOUT WIND STRESS

Figure 3 reveals an idealized conceptualization for a cross-section of fresh water encountering sea water. The integrity of the fresh water is maintained by assigning a nonpermeable, massless membrane as the interface between the fresh and sea water. The equation governing the pressure, P_O, that develops across the interface at depth h_O is

$$P_O = (\rho_S - \rho_O) \, g \, h_O, \tag{1}$$

where ρ_S is sea water density (kg m^{-3}),

ρ_O is fresh water density (kg m^{-3}),

g is gravitational acceleration (m s^{-2}), and

h_O is fresh water wedge depth (m).

If the resultant baroclinic flow were to proceed to its final rest state there would be a layer of fresh water on top of sea water (Figure 4). The potential energy, E, released in this process is given by

$$E = (\rho_S - \rho_O) \, g \, \Delta h \, \text{Vol}, \tag{2}$$

where Δh is distance the center of mass moves (m) and

Vol is the volume of the entire fresh water wedge (m^3).

In Figure 3 the center of mass of the fresh water layer is $h_O/3$. The height of the center of mass in the rest state (Figure 4) is $h_O/4$. Therefore, the change in height, Δh, is $h_O/12$. Substituting into equation (2),

$$E = (\rho_S - \rho_O) \, g \, h_O/12 \, \text{Vol}. \tag{3}$$

The exact value of the potential energy can be obtained by integrating over the entire volume of fresh water (Figure 5) so that,

$$E = (\rho_S - \rho_O) \, g \, L \, M \, h_O^2/144, \tag{4}$$

where L is the length of coastline (1300 km) and

15

Offshore ←

Coastal
Boundary

Fresh Water Layer

ρ_0

$h_0/3$

Center
Of Mass
Distance

Interface.
Between Fresh and
Sea Water

ρ_s

Sea Water Layer

h_0

M

ρ_0 - Density of Fresh Water (kg m^{-3})

ρ_s - Density of Sea Water   (kg m^{-3})

M - Cross-shelf Distance   (m)

h_0 - Fresh Water Depth at Coast (m)
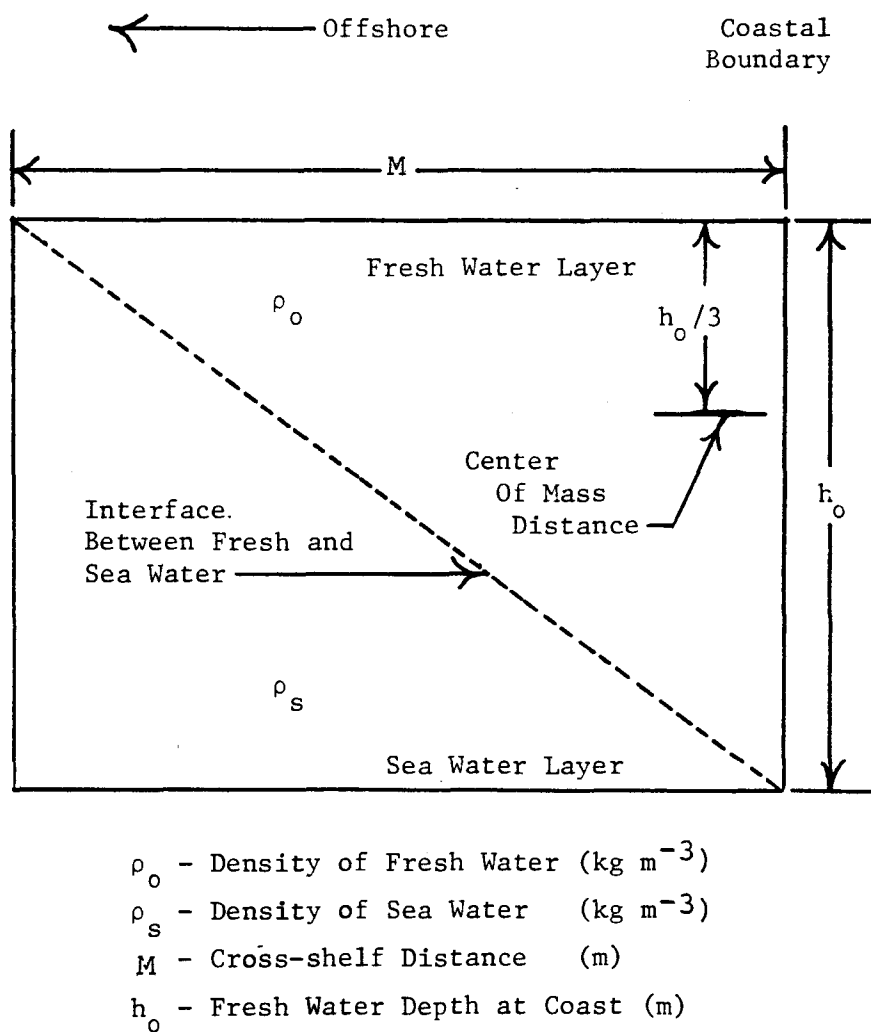
Figure 3 - Idealization of cross-shelf fresh water wedge.
View is looking westward. Resultant baroclinic
flow moves westward.

Offshore   Coastal
                                 Boundary

$\leftarrow$ ——————————— M ——————————— $\rightarrow$

ρ_o

$h_o/4$

Center of Mass Distance ⌐

Interface

ρ_s

h_o
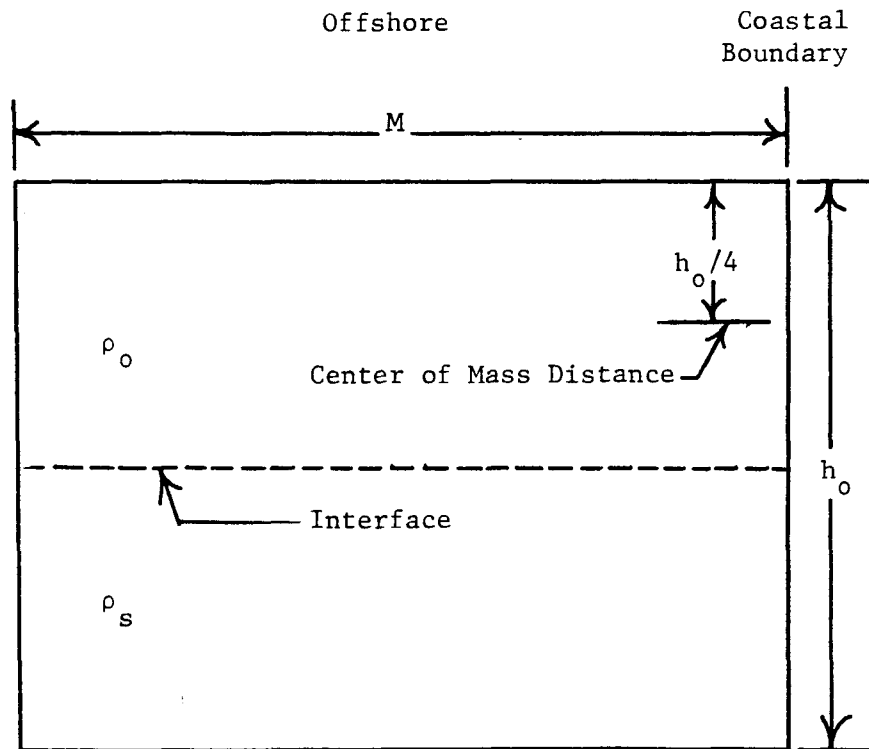
Figure 4 - Lowest energy state for fresh water. Center of
           mass in different position from Figure 3.
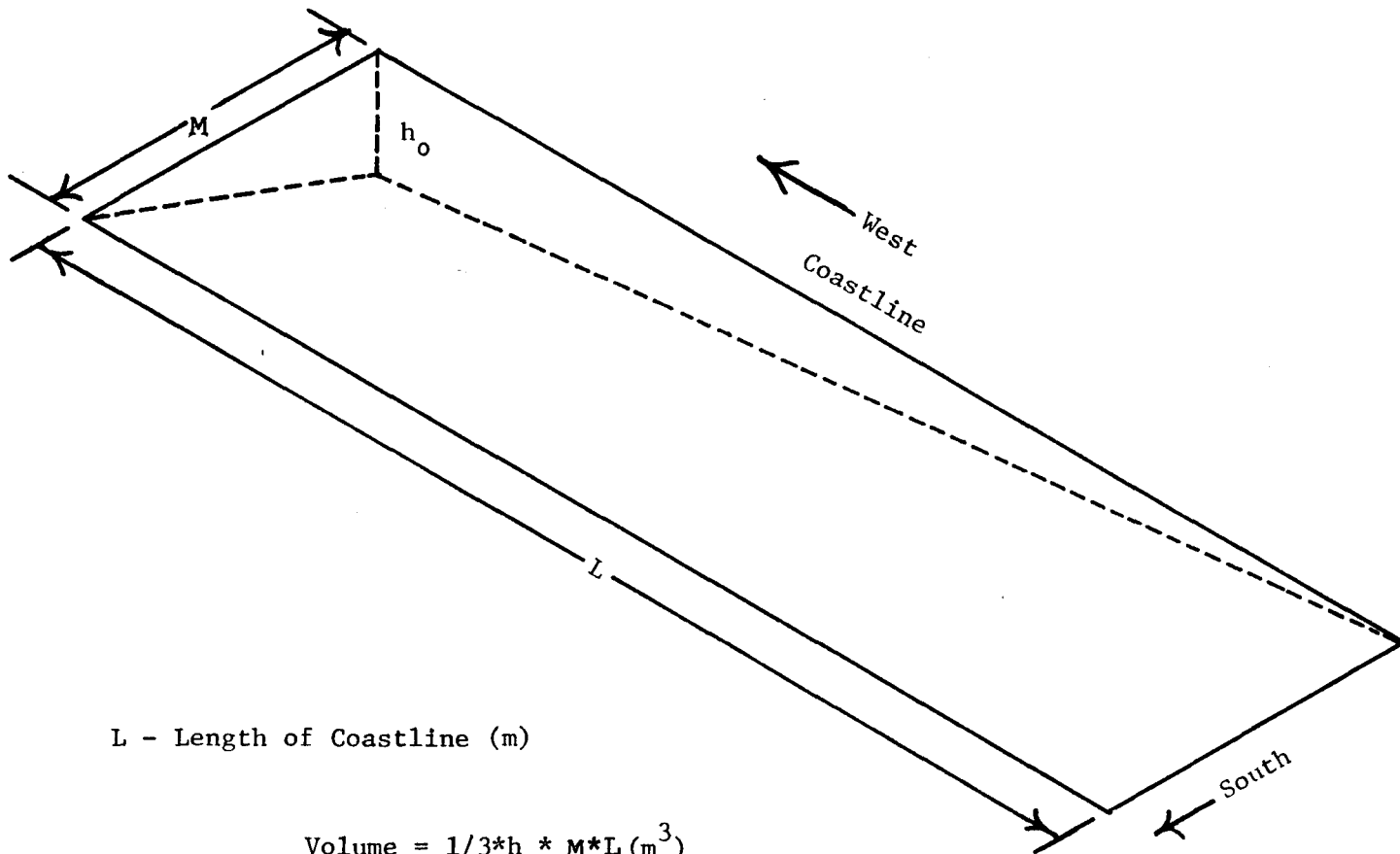
L - Length of Coastline (m)

Volume = $1/3*h_o * M*L$ (m^3)

Figure 5 – Three dimensional conceptualization of the entire (cross-shelf and long shore) extent of fresh water wedge.

M is the cross-shelf distance of fresh water (m).

Pedlosky (p.336, 1979) gives a theoretical value for the cross-shelf fresh water distance;

$$M = (g(\rho_S - \rho_O) \, d/2/\rho_a)^{1/2}/f, \qquad (5)$$

where **f** is Coriolis parameter (s^{-1}),

　　d is depth of water column (200 m), and

　　ρ_a is average fluid density (1012.5 kg m^{-3}).

ρ_S is considered to be an infinite oceanic source and ρ_O a finite source, since the fresh water discharge is finite and much smaller than the large reservoir of oceanic water. The assumption about no mixing is inconsequential here since the absence of wind dictates no large scale mixing.

The following concept for dealing with power is not new in physical system analysis (Shearer et al., 1967). An analogy can be made between electrical and fluid systems. In electrical systems, a common concept for storing energy is the capacitor. The capacitor stores electrical energy by virtue of a potential charge difference (voltage). The power that can be obtained from the capacitor is the product of the flow rate of charge (current) and the voltage. The concept of the fluid capacitor is introduced as a method of storing energy due to a pressure differential. Fluid pressure and flow rate are respectively analogous to electrical voltage and current. Thus, the baroclinic power, P_O, can be expressed, Shearer et al. (p. 631, 1967), by combining the flow rate, Q, and the pressure, p_O,

$$P_O = p_O \, Q. \qquad (6)$$

Equation (6) describes the baroclinic alongshore power produced by the

cross-shelf pressure gradient. For this case, the baroclinic fresh water transport is equal to the total fresh water discharge. Due to the rotation effects, the fresh water flows perpendicular to the pressure gradient.

The crux of the problem now depends upon finding an expression for the fresh water wedge depth in terms of the fresh water discharge. The following equation is another expression that describes the baroclinic alongshore power of the fresh water layer,

$$P_O = \rho_a/2 \; A_{nw} \; v^3, \tag{7}$$

where A_{nw} is the area of the fresh water wedge (m^2) and

v is alongshore velocity of fresh water layer ($m \; s^{-1}$).

Since the system is constrained into two layers, the cross-shelf density gradient is a constant over the depth of the fresh water wedge. The alongshore velocity of the fresh water layer will be considered to be uniform,

$$v = Q/A_{nw}. \tag{8}$$

Substituting equation (8) into equation (7) gives,

$$P_O = \rho_a/2 \; Q^3/A_{nw}^2 \tag{9}$$

$$A_{nw} = M \; h_O/2. \tag{10}$$

Using equations (10), (9), (6), (1) and solving for the fresh water wedge depth yields the following expression:

$$h_O = (2\rho_a Q^2/(\rho_s - \rho_o)/g/M^2)^{1/3}. \tag{11}$$

Using equations (11), (6), and (1) produces an expression for the alongshore baroclinic power;

$$P_O = Q^{5/3}(2\rho_a(g(\rho_s - \rho_o)/M)^2)^{1/3} \tag{12}$$

Thus, the power is a non-linear function of the fresh water discharge

(Figure 6).

FRESH WATER FORCING WITH WIND STRESS

It is now reasonable, having established some basic concepts of the model, to investigate the coupling with a steady wind. For our situation, we will consider an easterly, alongshore wind. Ekman (1905) determined that for a rotating system, a wind blowing across a water surface will induce water velocities, called wind drift currents, both parallel and perpendicular to the wind direction. Thus, the wind, in addition to accelerating the water alongshore, will move the fresh water shoreward, constraining it into a narrow band.

Figures 7 and 8 show the orthonormal wind drift velocity components as a function of depth, for low and high wind speeds. The cross-shelf, U_{wd}, and alongshore, V_{wd}, wind drift currents are prescribed as a function of depth, z, by the following equations from Neumann & Pierson (p. 1974, 1966),

$$U_{wd} = \alpha \sinh(k) \cos(k) - \gamma \cosh(k) \sin(k), \qquad (13)$$

$$V_{wd} = \alpha \cosh(k) \sin(k) + \gamma \sinh(k) \cos(k), \qquad (14)$$

$$K = B/sqr2 \ (d-z), \qquad (15)$$

$$sqr2 = (2)^{1/2}, \qquad (16)$$

$$B = (f \ \rho_a/A)^{1/2}, \qquad (17)$$

where A is the vertical eddy viscosity (kg m^{-1} s^{-1}),

$$A = 0.1825 \ W^{5/2}, \qquad (18)$$

where W is the wind velocity (m s^{-1}),

$$\alpha = C_o/T_{ang}(\cosh(E) \cos(E) + \sinh(E) \sin(E)), \qquad (19)$$

$$\gamma = C_o/T_{ang}(\cosh(E) \cos(E) - \sinh(E) \sin(E)), \qquad (20)$$

$$C_o = \tau D/A/ \ , \qquad (21)$$
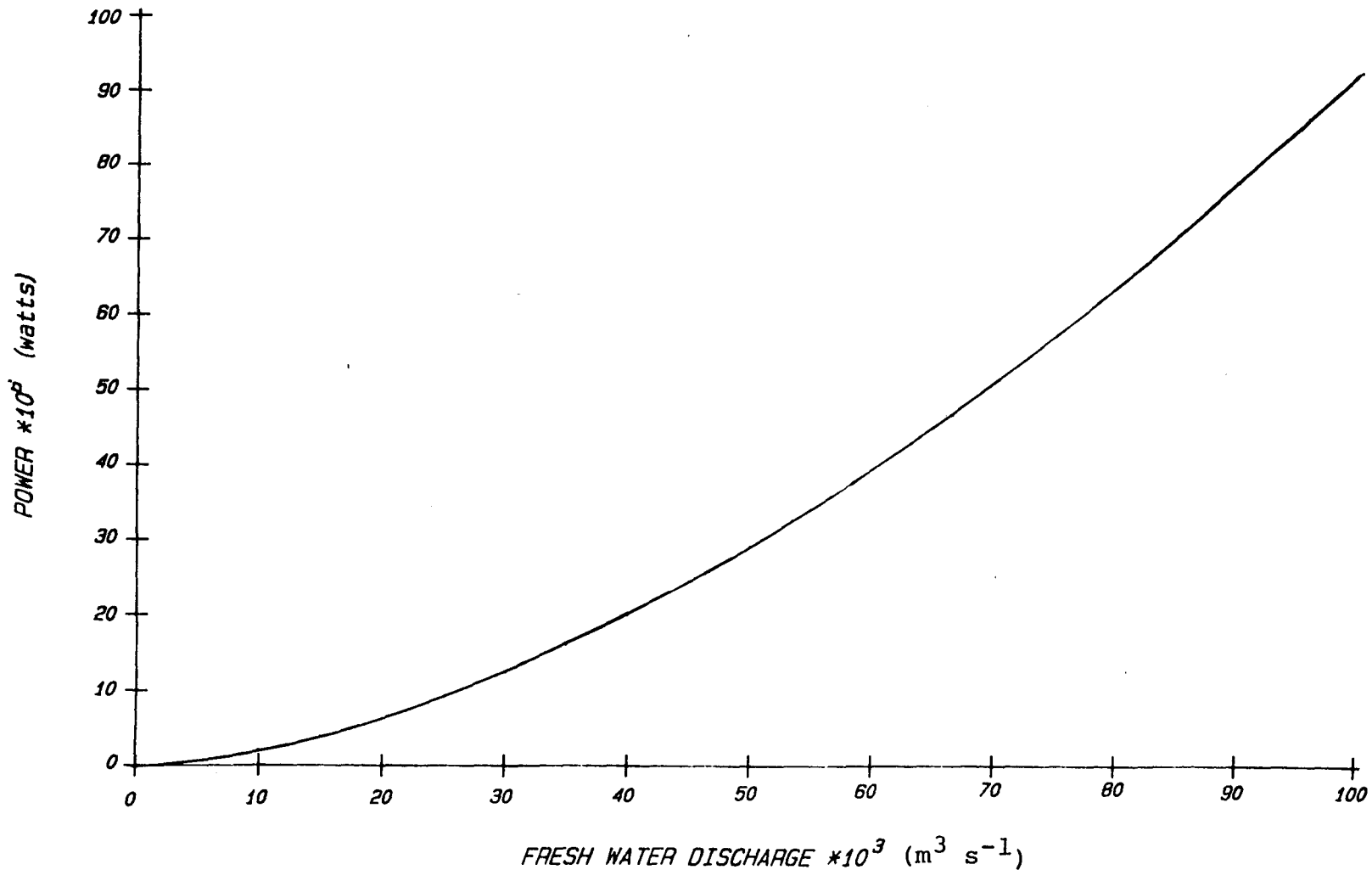
Figure 6 – Alongshore baroclinic power for the fresh water wedge versus fresh water discharge.
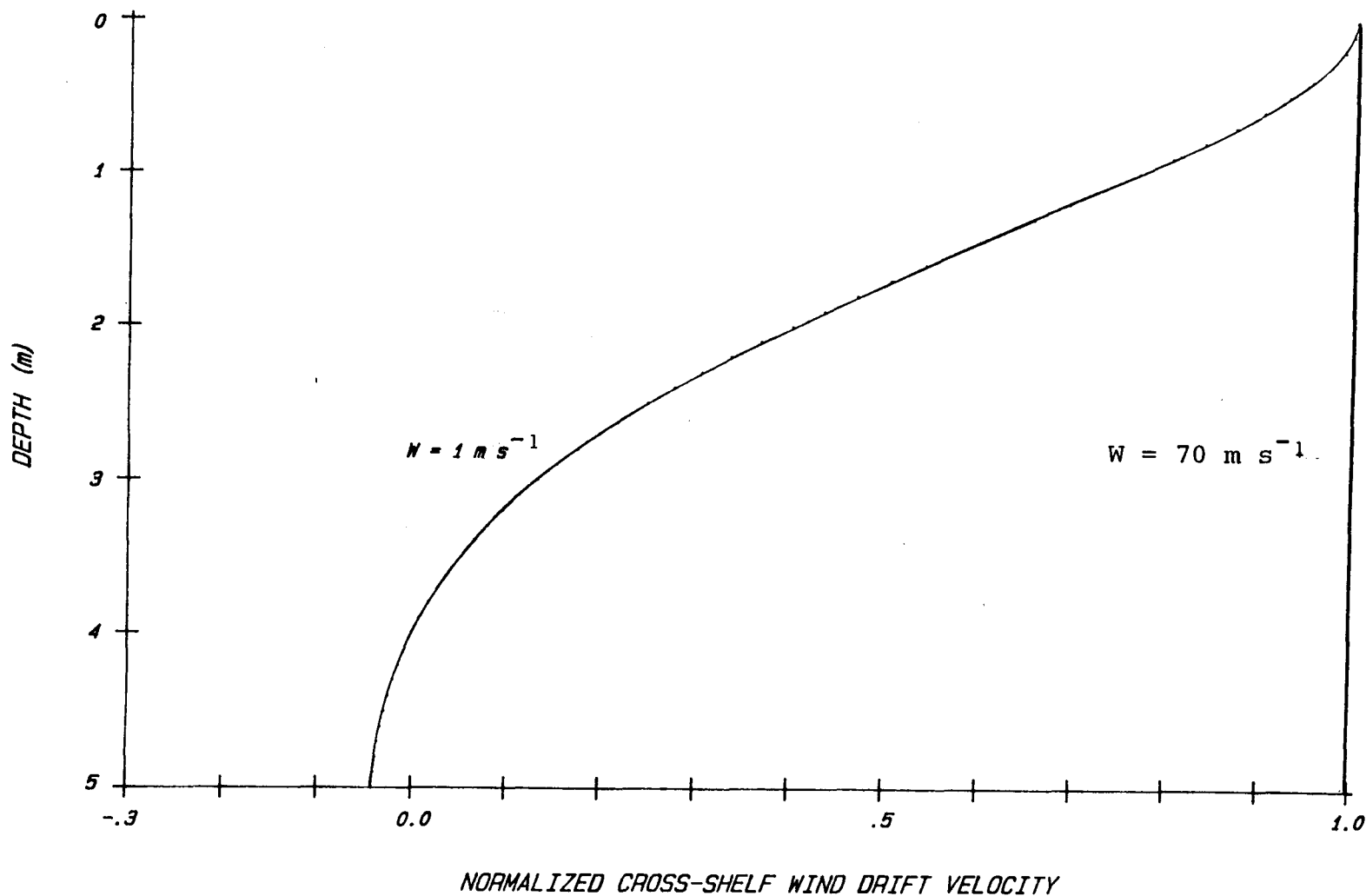
Figure 7 - Vertically resolved, cross shelf, wind drift currents normalized to the surface value for wind speeds of 1 m s^{-1} and 70 m s^{-1}.
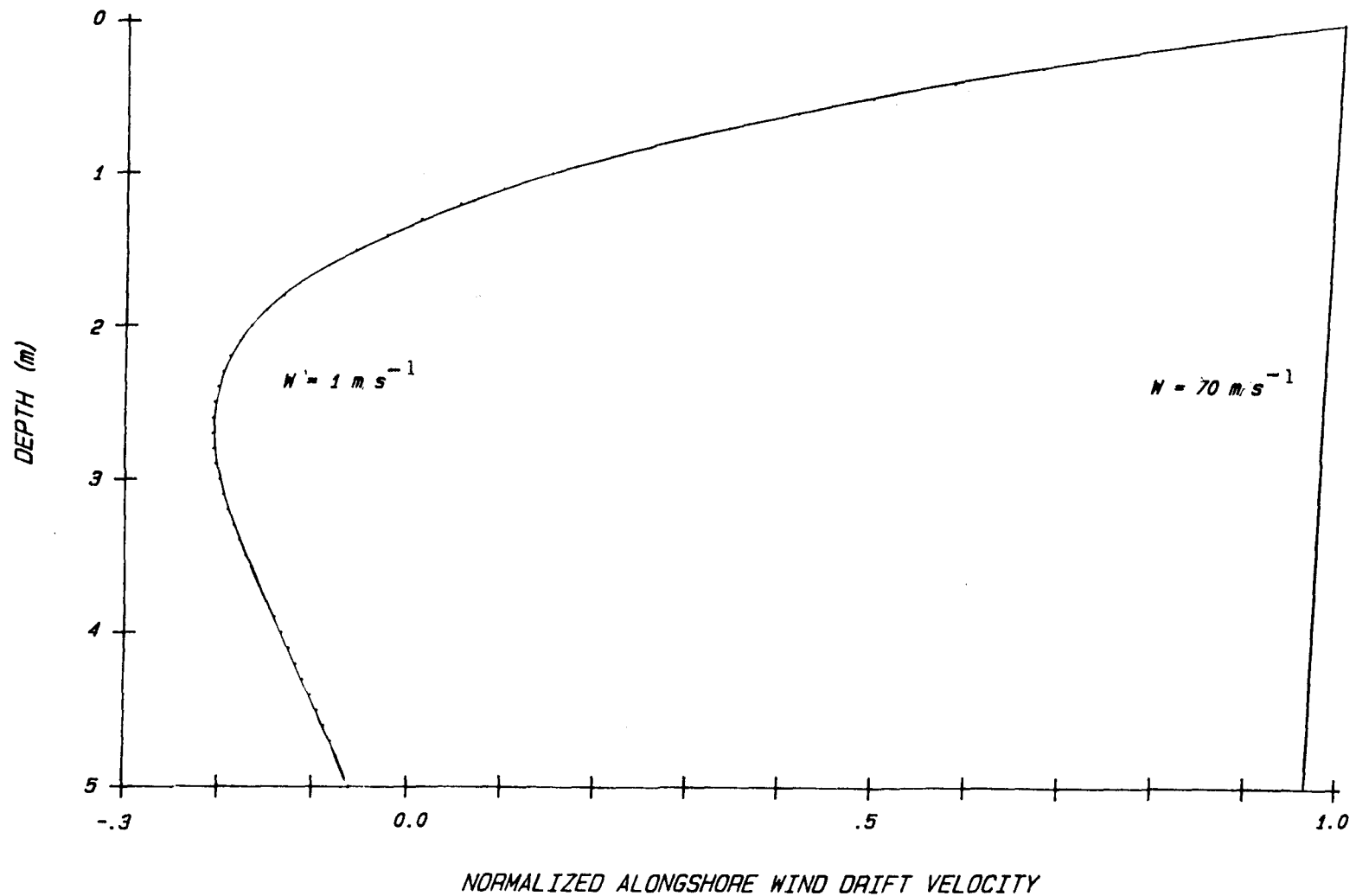
Figure 8 – Vertically resolved, alongshore, wind drift currents normalized to the surface value for wind speeds of 1 m s^{-1} and 70 m s^{-1}.

and τ is the shear stress due to the wind (pascals).

From Pond and Pickard (p.88, 1978),

$$\tau = 1.8*10^{-3} \ W^2, \tag{22}$$

where **D** is the depth of frictional influence (m), and

$$D = \pi(2A/ \ \rho_a/f)^{1/2}. \tag{23}$$

From Neumann and Pierson (p. 194, 1966)

$$T_{ang} = \cosh(2E) + \cos(2E), \text{and} \tag{24}$$

$$E = B \ d/srq2. \tag{25}$$

In addition to the shoreward movement of fresh water, a sea surface slope, of angle β, develops perpendicular to the shore. There is also an alteration of the fresh water wedge depth, **h**, which is depicted in Figure 9.

The wind drift currents extend downward through the water column in a rotary, exponentially decaying fashion. However, we shall only be concerned with the top several meters of the water column since, for purposes of the model, this is the regime dominated by the fresh water.

For the steady-state situation, the total alongshore transport of fresh water must equal the total fresh water discharge from the coast. This assumes no net transport in the cross-shelf direction. Figure 10 shows the cross-sectional areas occupied by the baroclinic, Q_{bc}, and wind drift, Q_{wd}, transports. Since the total alongshore transport of fresh water must equal the fresh water discharge, the discharge and transports can be related by

$$Q = Q_{bc} + Q_{wd} \tag{26}$$

The baroclinic transport can be expressed by rewriting equation (8) with the new variables for the wind driven case,
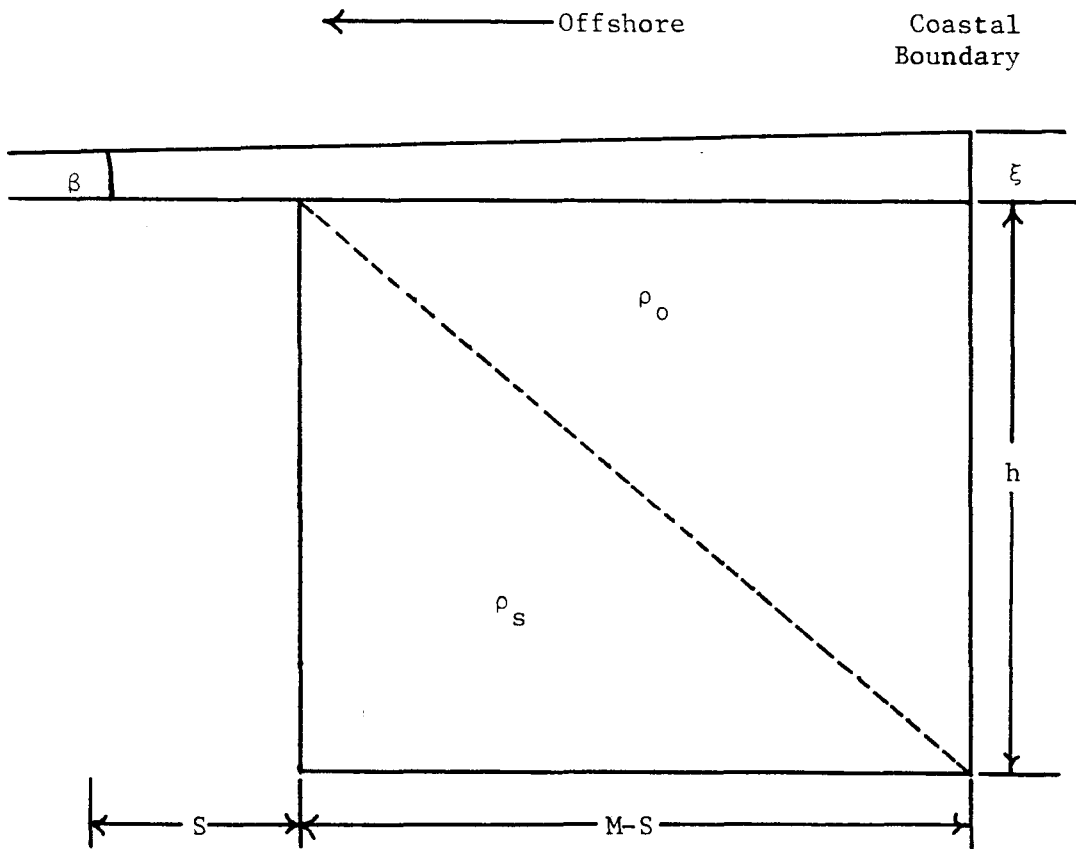
ξ – Sea Height at Coast (m)

β – Angle of Sea Surface (rad)

S – Distance Fresh Water Moved Shoreward Due to Wind (m)

h – Altered Fresh Water Depth at Coast (m)

Figure 9 – Easterly (into the paper) wind produces shoreward, Ekman transport and a cross-shelf sea surface slope. Depth of fresh water layer is altered.

27

Figure 10 - Areas through which baroclinic and wind drift transports flow.

$$Q_{bc} = V_{bc} A_{bc} \qquad (27)$$

where V_{bc} is the baroclinic alongshore velocity $(m\ s^{-1})$,

A_{bc} is the area for the baroclinic transport (m^2),

$$A_{bc} = (M-S)\ h/2, \qquad (28)$$

and S is the distance that the fresh water is moved shoreward (m).

Equations (6) and (7) can be rewritten using the new variables,
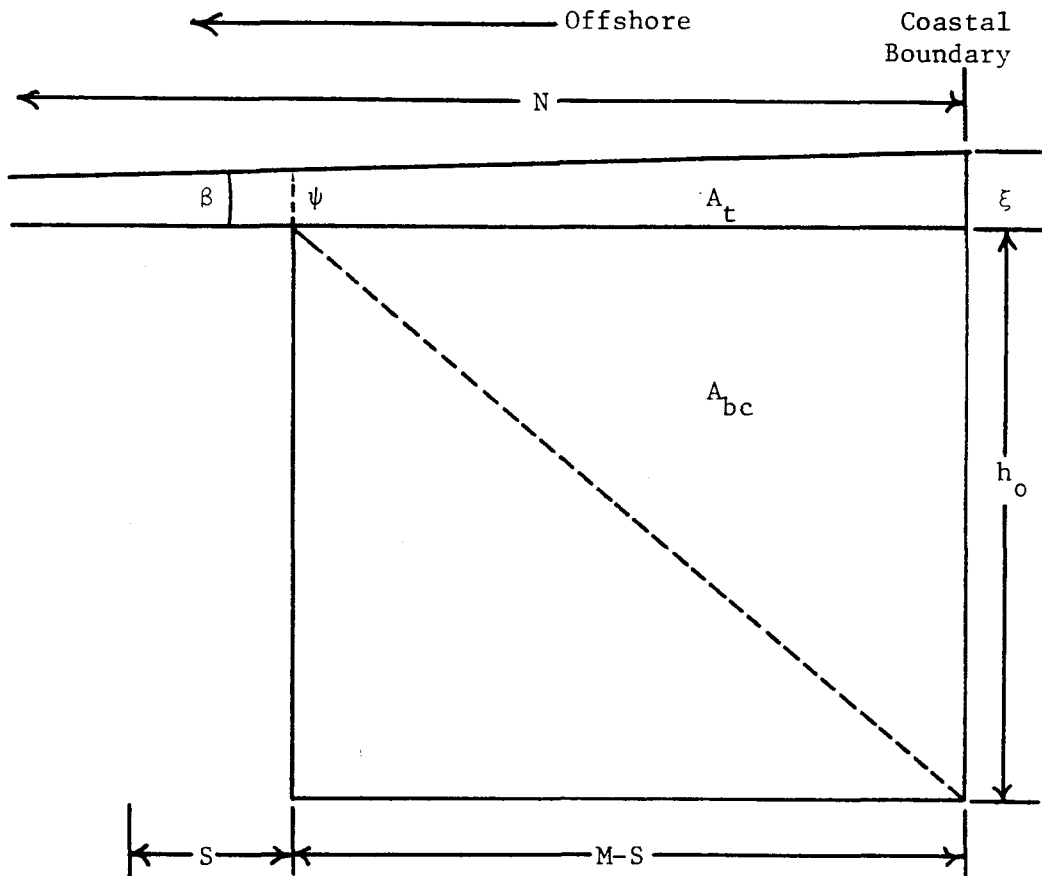
$$P_{bc} = (\rho_s - \rho_o)\ g\ h\ Q_{bc}, \qquad (29)$$

$$P_{bc} = \rho_a/2\ Q_{bc}\ V_{bc}^2, \qquad (30)$$

where P_{bc} is the baroclinic alongshore power (w).

Equations (29) and (30) can now be used to solve for the baroclinic alongshore velocity;

$$V_{bc} = (2(\rho_s - \rho_o)/\rho_a\ g\ h)^{1/2} \qquad (31)$$

Substituting equations (31) and (28) into equation (27) yields the following expression for the baroclinic fresh water transport,

$$Q_{bc} = (M-S)h^{3/2}\ (g(\rho_s - \rho_o)/2/\rho_a)^{1/2}. \qquad (32)$$

The wind drift fresh water transport will be the sum of the transports through the sea slope wedge area, A_t, and the wedge area occupied by the baroclinic transport,

$$Q_{wd} = V_s A_t + \int\int V_{wd}\ dzdx \qquad (33)$$

where V_s is the surface wind drift current $(m\ s^{-1})$, and

$$V_s = \alpha \cosh(E)\ \sin(E) + \gamma \sinh(E)\ \cos(E). \qquad (34)$$

The surface velocity is used because the wedge depth is very small and the velocity will vary only $0.01\ m\ s^{-1}$ over the depth of the wedge for low wind speed. For high wind speed the variation in velocity over the wedge depth becomes less (Figure 8), which increases the accuracy of the approximation. The derivation of A_t can be found in appendix A.

$$A_t = \tan(\beta)/2 \ (N^2 - (N-M+S)^2),$$ (35)

where **N** is the seaward sea slope extent (m), and

$$N = (g \ d)^{1/2}/f.$$ (36)

The integration of the alongshore wind drift current through the baroclinic area yields,

$$V_t \ (M-S)/2/C = \iint V_{wd} \ dzdx$$ (37)

$$V_t = (\alpha+\gamma) \ \sinh(E) \ \sin(E) - (\alpha-\gamma) \ \cosh(E) \ \cos(E) +$$

$$(\gamma(\cosh(J) \ \sin(J) - \cosh(E) \ \sin(E)) + \alpha(\sinh(E) -$$

$$\sinh(J) \ \cos(J)))/c/h,$$ (38)

$$J = E-Ch, \ \text{and}$$ (39)

$$C = B/sqr2$$ (40)

Using equations (32), (33), (34), (35), (36), (37), and (38) yields an expression for the cross-shelf distance, **S**, in terms of the wedge depth, **h**,

$$S = (-b+ (b^2-4ac)/2/a,$$ (41)

$$a = V_s/2 \ \tan(\beta),$$ (42)

$$b = h^{3/2} \ B_g + (N-M)V_s \ \tan(\beta) + V_t/2,$$ (43)

$$c = M((M-2 \ N) \ V_s/2 \ \tan(\beta) - h^{3/2} \ B_g - V_t/2) + Q,$$ (44)

$$B_g = ((\rho_s - \rho_o)/\rho_a/2 \ g)^{1/2}$$ (45)

It is now appropriate to introduce a power balance. The baroclinic power of the induced coastal current must be the sum of the baroclinic power without wind and the power provided by the wind, P_w:

$$P_{bc} = P_o + P_w$$ (46)

It should be recalled that the expression for P_o is given by equation (12). The power from the wind can be determined by integrating the cube of the cross-shelf wind drift velocity over the wedge area (Figure 11).
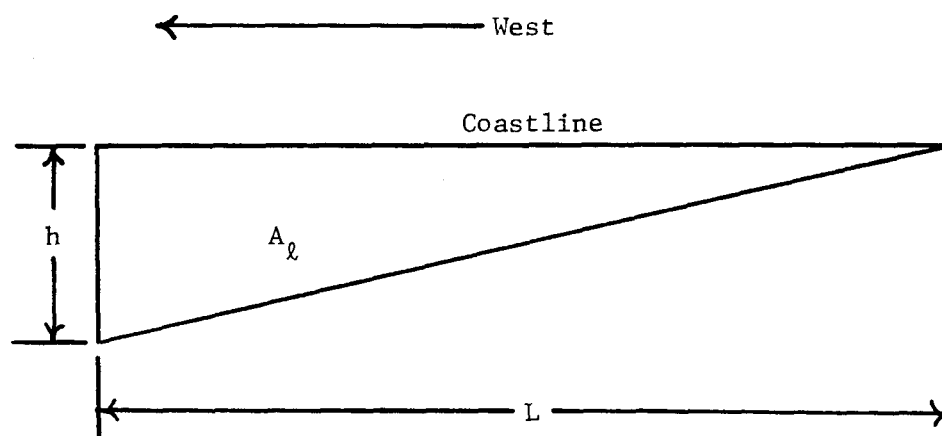
A_ℓ – Longshore Fresh Water Wedge Area (m^2)

Figure 11 – Fresh water wedge as viewed by looking directly
North, perpendicular to the coast.

It should be noted that the wedge area considered here is orthogonal to the one used for the transport scheme. The fresh water depth is considered to be a linear function of coast length. Thus, the power is given by:

$$P_w = \rho_a/2 \int\int U_{wd}{}^3 dzdx . \tag{47}$$

Due to its voluminous extent, the expression for P_w is listed in appendix B.

Combining equations (12), (29), (32), (41), (42), (43), (44), (45), (46), and (47) yields an expression for the fresh water depth, **h**, in terms of the independent parameters of wind speed, **W**, and fresh water discharge, **Q**,

$$h^{5/2}(M-S)(D_g{}^{3/2}/2/\rho_a)^{1/2} = Q^{5/3} C_{on} + P_w, \tag{48}$$

$$C_{on} = (2\rho_a(g(\rho_s-\rho_o)/f)^2)^{1/3} , \text{ and} \tag{49}$$

$$B_g = (\rho_s-\rho_o)g. \tag{50}$$

Unfortunately, **h** is not in a form conducive to an explicit solution. Therefore, a numerical iteration scheme, binary chop (interval halving), is used to determine the value of **h**. Once **h** is known it can be substituted into the desired expressions to evaluate various parameters of the current.

By applying the inputs of fresh water discharge, **Q**, and wind speed, **W**, the values of baroclinic power, P_{bc}, and fresh water transport, Q_{bc}, can be computed for the induced coastal current. These relationships can be expressed by the following generic equations,

$$P_{bc} = F(Q,W) , \text{ and} \tag{51}$$

$$Q_{bc} = F(Q,W) . \tag{52}$$

Chapter III   RESULTS AND DISCUSSION

Various combinations of fresh water discharge and wind speed were
applied to the model.   The discharge values range from   10000 - 90000
$m^3 s^{-1}$ and the wind speed values range from 2 - 70 m s^{-1} (approximately
4 - 140 knots).   In comparison, the yearly mean flow rate of the
Mississippi River is 18000 $m^3 s^{-1}$.

The wind dependent response for baroclinic fresh water transport,
fresh water wedge depth, alongshore baroclinic power, alongshore baro-
clinic velocity of the fresh water layer, and the baroclinic fresh water
wedge area normal to the coast are shown in Figures 12 to 16.   The
yearly mean flow rate (23000 $m^3 s^{-1}$) for this coastline was the fresh
water discharge value used in the afore mentioned cases.   The
nonmonotonic structure of the distributions in the afore mentioned
figures results from wind drift currents in a water column of finite
depth.   The behavior of the normalized wind drift, surface velocity
components Us and Vs in the cross-shelf, and alongshore directions are
illustrated in Figure 17.   An increasing wind speed increases the Ekman
depth, the depth that the water is frictionally influenced by the wind.
The ratio of bottom depth to Ekman depth causes a deviation, from the
infinite depth case, in the wind drift profiles.   The resulting peak in
the cross-shelf component (Figure 17) would not be present if the water
was infinitely deep.   This peak plays an important role in shaping the
behavior of the parameters to be discussed.

The cross-shelf distribution has a bell shape similar to the
baroclinic power distribution (Figure 14).   As can be seen from equation
(46), the resultant alongshore baroclinic power, P_{bc}, is the sum of the

32
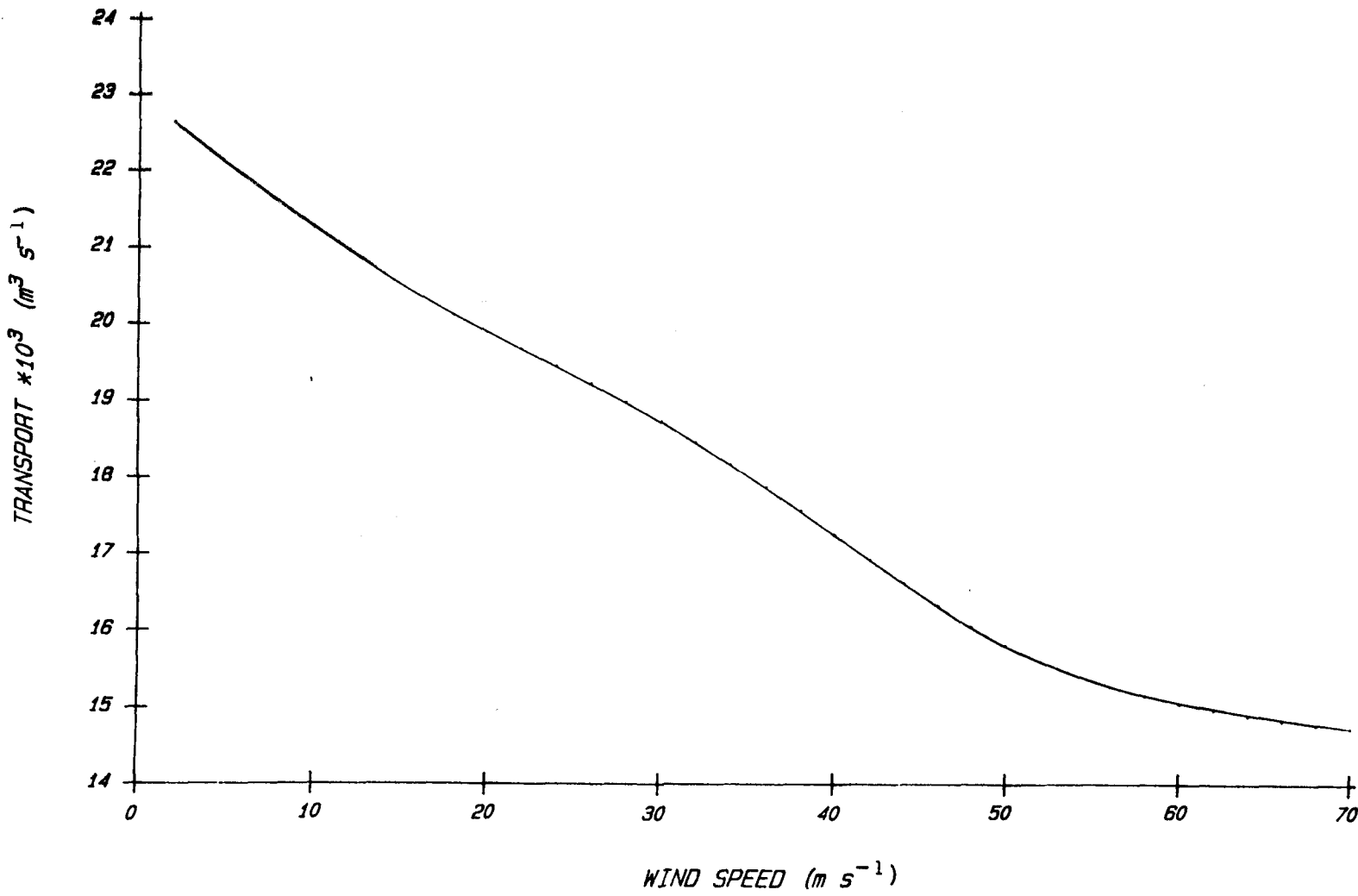
Figure 12 – Alongshore transport of fresh water as a function of wind speed, for a discharge of 23000 m^3 s^{-1}.
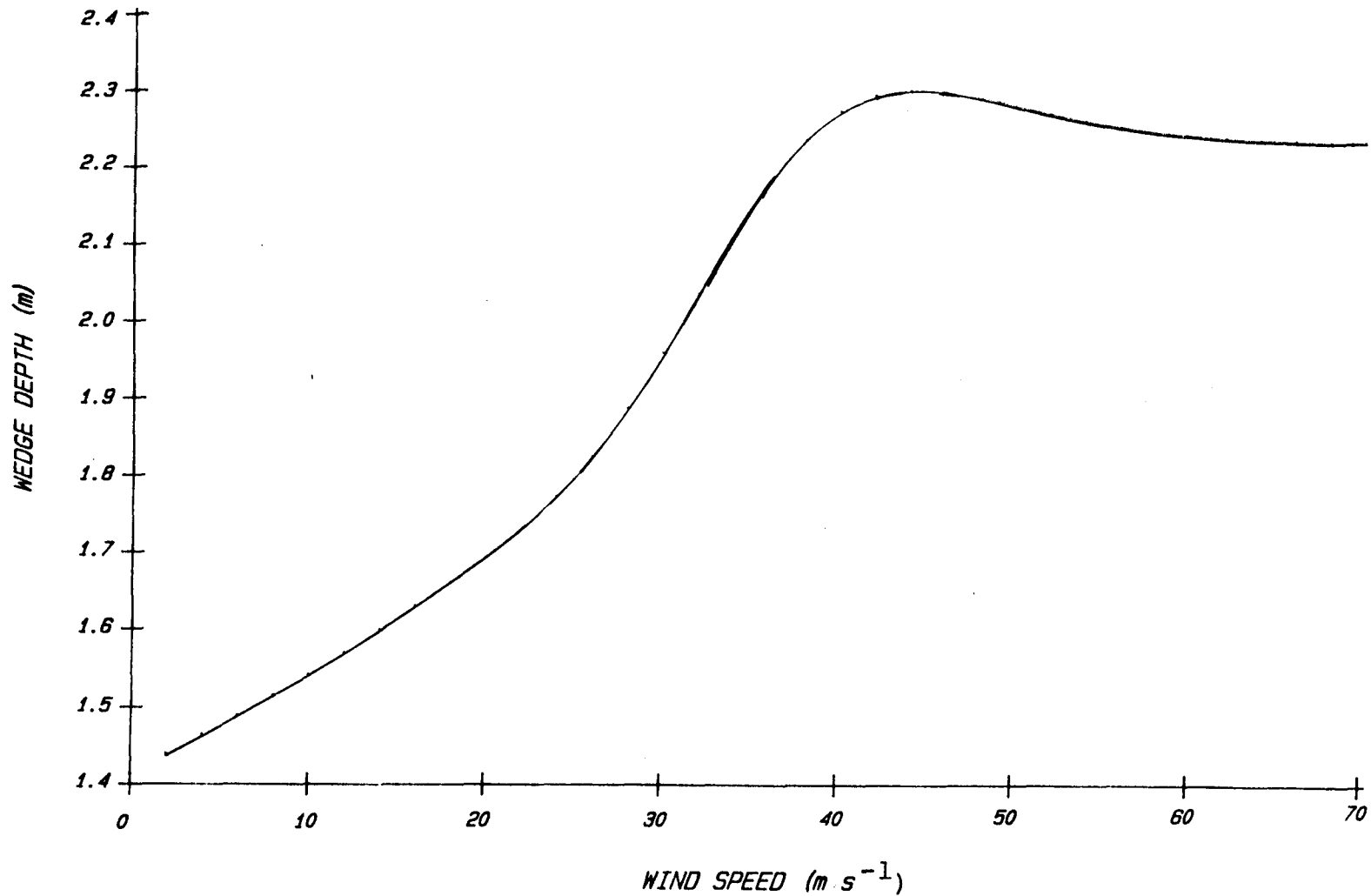
Figure 13 – Fresh water wedge depth at coast as a function of wind speed, for a discharge of 23000 m^3 s^{-1}.
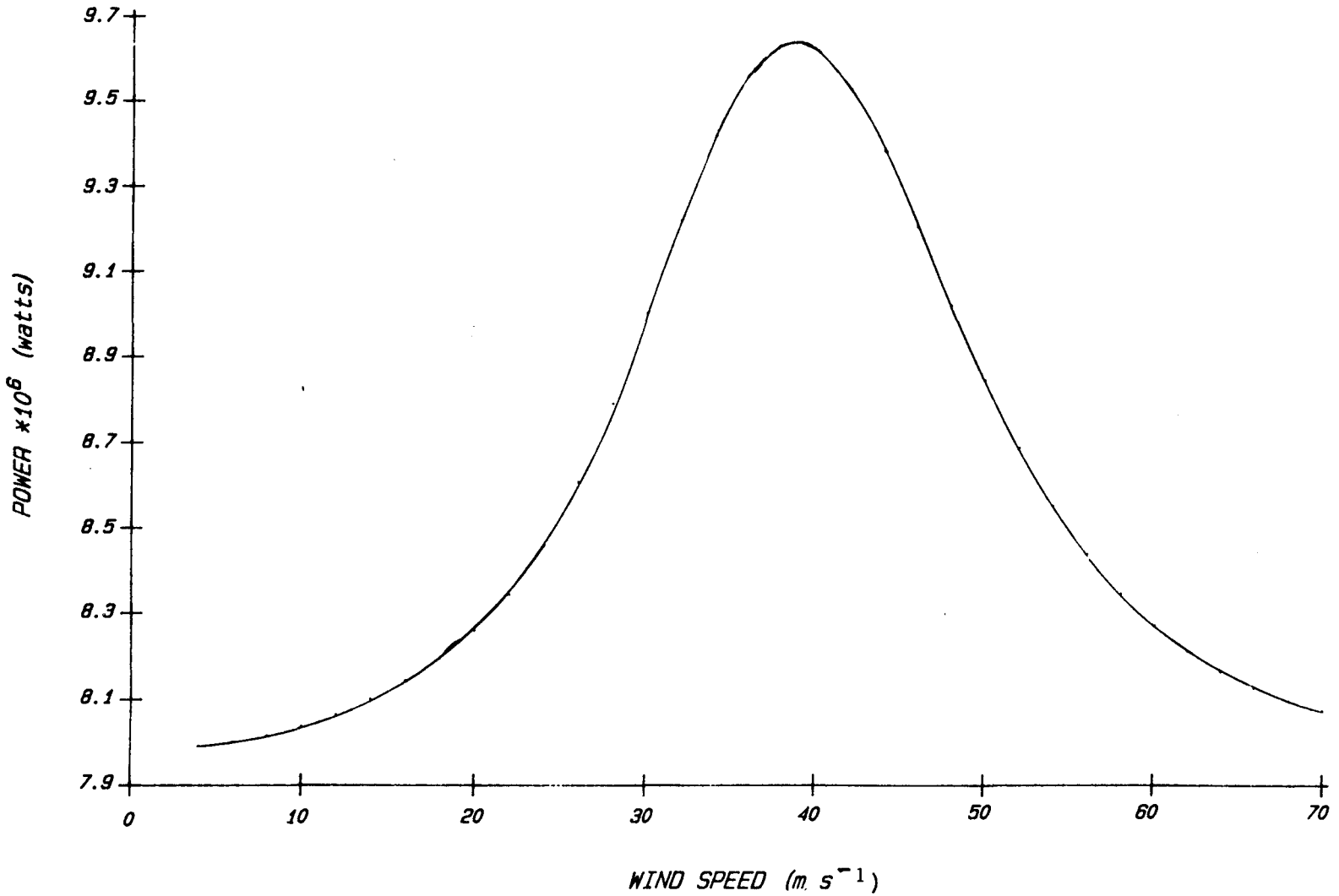
Figure 14 – Alongshore, baroclinic power for the fresh water as a function of wind speed, for a discharge of 23000 m^3 s^{-1}.

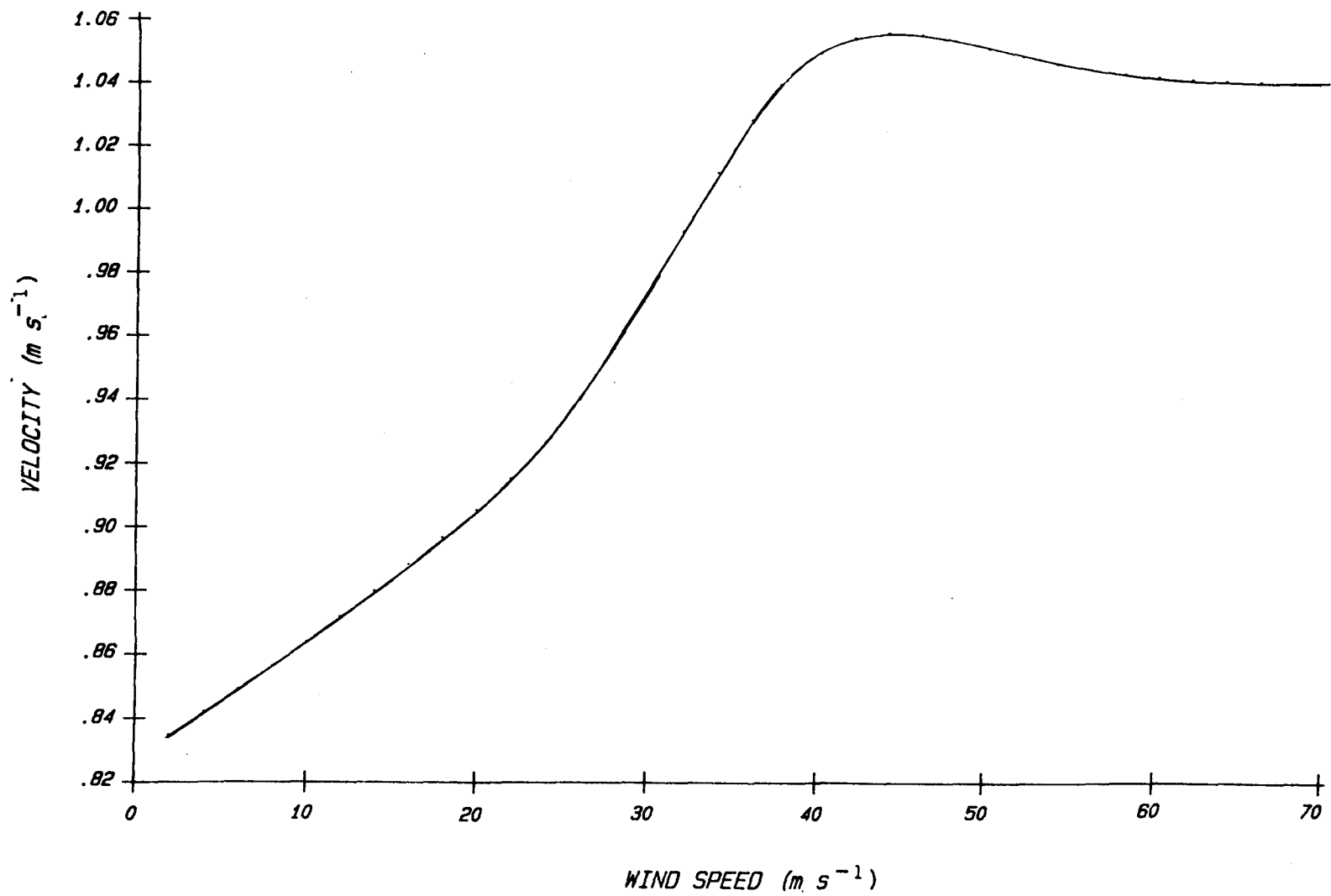Figure 15 – Alongshore, baroclinic velocity of fresh water wedge as a function of wind speed, for a discharge of 23000 m^3 s^{-1}.
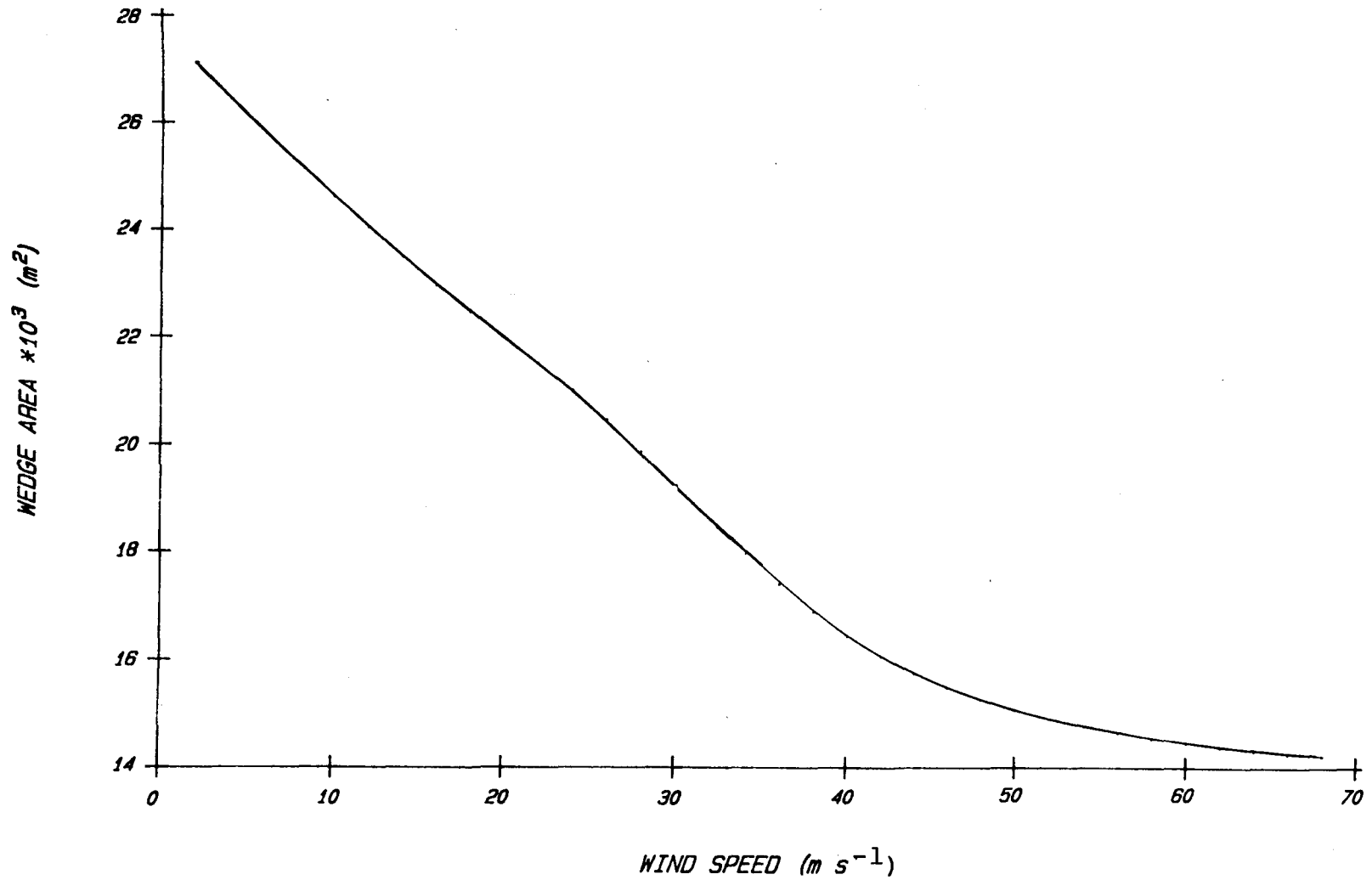
Figure 16 – Cross-sectional area of the baroclinic fresh water wedge as a function of wind speed, for a discharge of 23000 m^3 s^{-1}.
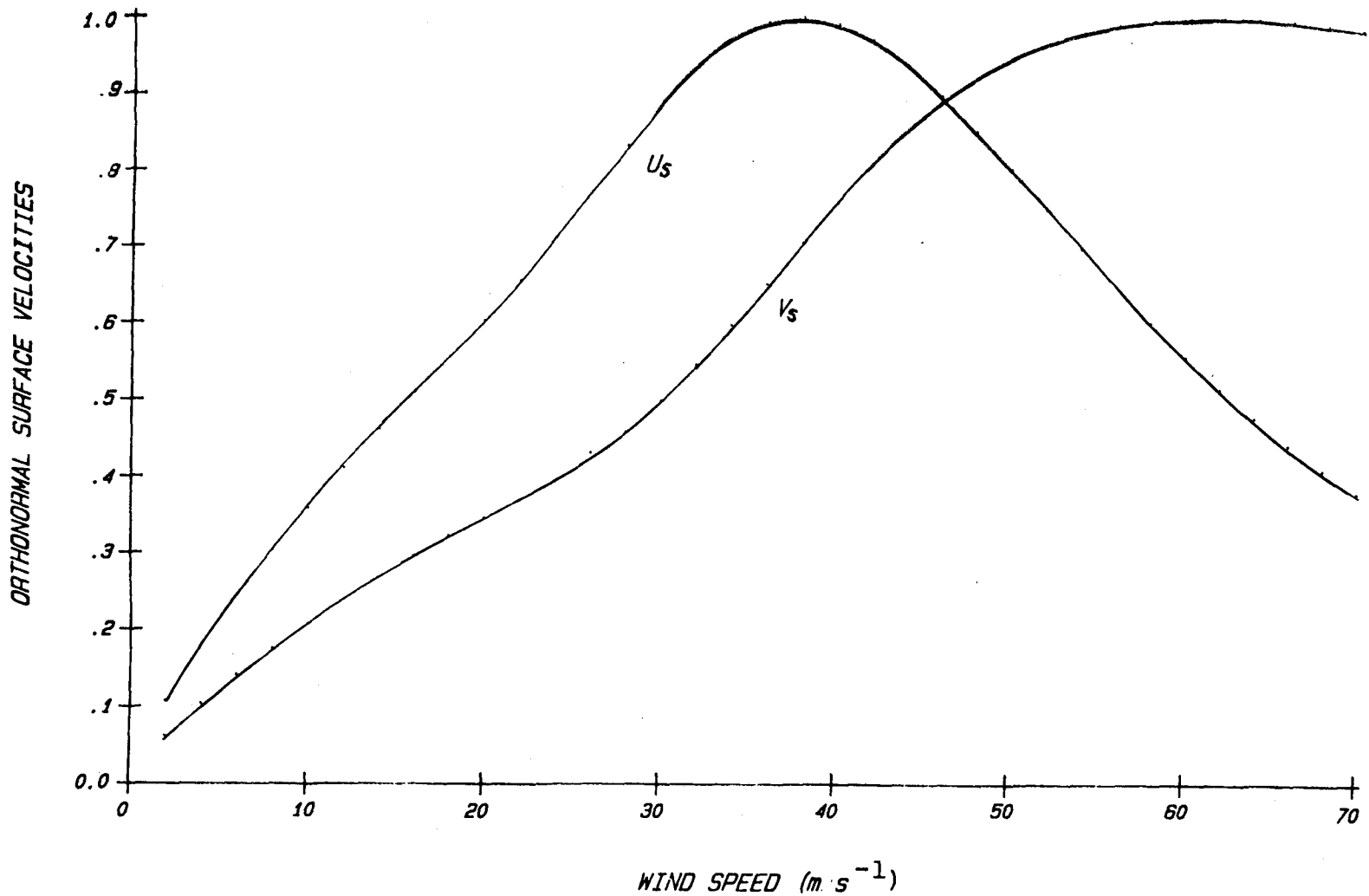
Figure 17 – Surface velocities for cross-shelf and alongshore wind drift currents, normalized to their maximum values, respectively.

baroclinic power without wind, P_o, and the power due to the cross-shelf wind drift currents, P_w. P_o is a constant for a given value of discharge. It follows that P_{bc} should reflect the behavior of P_w. Since P_w is a function of the cross-shelf velocity, P_{bc} must have a distribution similar to the cross-shelf wind drift currents. It is slightly different because it is also a function of the cross-sectional baroclinic area, which also changes as a function of wind speed.

The behavior of the baroclinic transport (Figure 12) can be reasonably represented by the alongshore surface velocity profile (Figure 17). The wind drift transport is continuously increasing in response to the increasing wind drift velocity. However, it is noticed (Figure 17) that there is a peak in the alongshore velocity distribution at high wind speed. There is a slight decrease at higher wind speeds. The wind drift transport has a very slight increase at high wind speed but does not decrease. This is because the sea surface slope increases as a function of wind speed (Figure 18), causing area A_t to increase, increasing Q_{wd}. As can be seen from equation (26), a constant discharge, Q, will require any change in wind drift transport, Q_{wd}, to be balanced by a change in baroclinic transport, Q_{bc}. Therefore, the increase in Q_{wd} must result in a decrease in Q_{bc} (Figure 12).

Having justified the distribution for P_{bc} and Q_{bc} as a function of wind speed, the distribution of the fresh water wedge depth, h, as a function of wind speed can be readily understood by referring to equation (29). The depth is the ratio of power divided by transport modified by a constant. Since the power distribution is peaked and the transport distribution is monotonic, we should expect to find a peak in
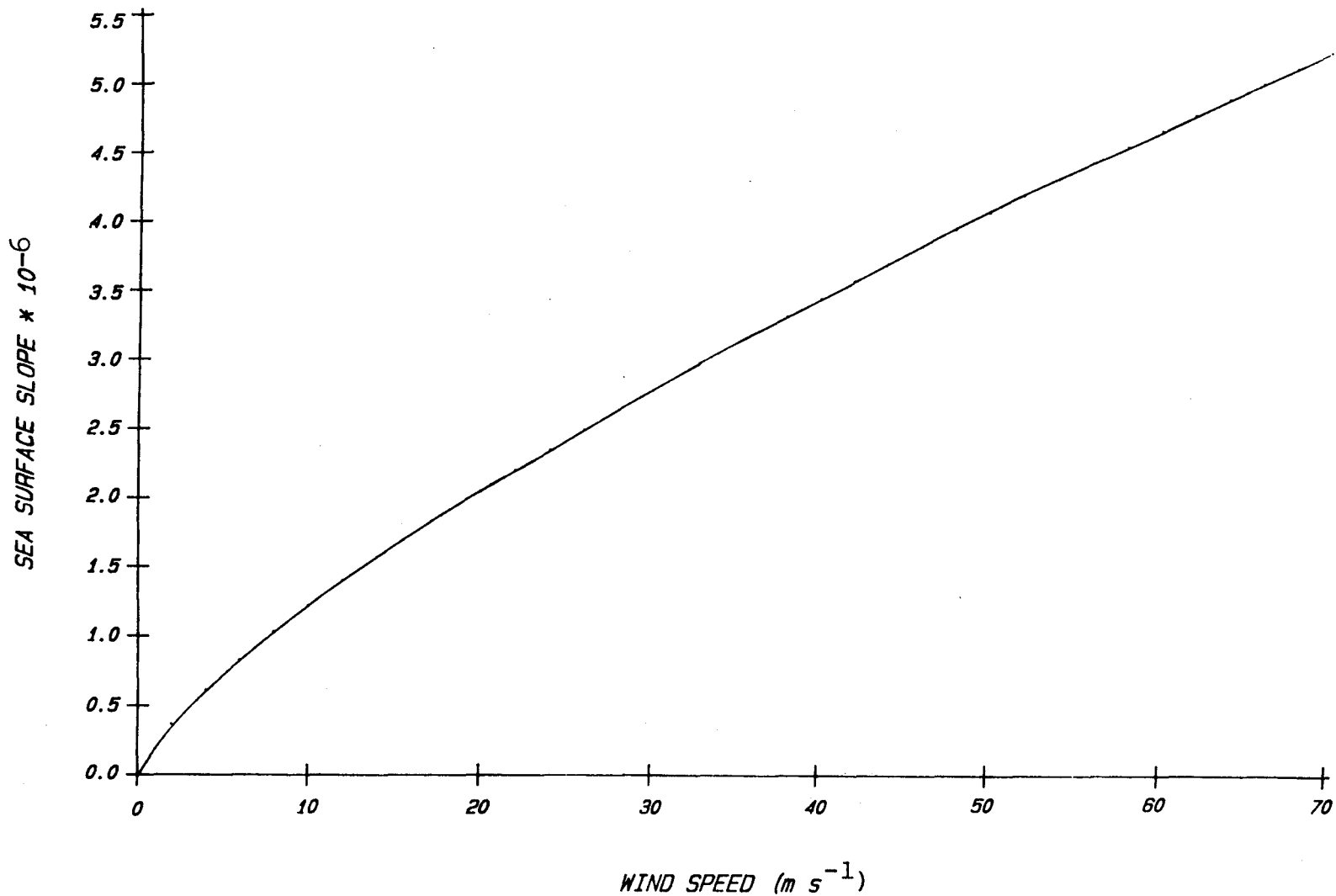
Figure 18 – Sea surface slope, perpendicular to the coast, as a function of wind speed.

the distribution for **h**. The distributions for P_{bc} and **h** used in concert with the appropriate equations can explain the profiles of Figures 15 and 16.

The main point to be gleaned from the above examples is that the structure seen in the distributions is due to the behavior of the cross-shelf and alongshore wind drift currents as a function of wind speed. By definition, our problem has dealt with a layer of fresh water moving with uniform velocity. Therefore, there can not be any structure imposed by the baroclinic current. For the windless case, the lack of structure is depicted in Figure 6 by the smooth, non-oscillating, monotonic curve for alongshore baroclinic power as a function of fresh water discharge.

The relationship for various system parameters as a function of wind speed and fresh water discharge is shown in Figures 19 to 25. The normalized power distribution (Figure 19) shows a definite peak for all the curves occurs at the same wind speed. The change in discharge affects the relative percentage with which the wind alters the power. If some perturbation on a system is small compared to the major process in the sysstem, the effect of the perturbation should be small. Increased values of discharge tend to smooth the distributions, removing the structure. This effect can be seen for the distributions of wedge depth and alongshore velocity (Figures 21 and 22). From Figure 20 it appears that there is increased structure in the transport distribution due to increased values of discharge as a function of wind speed. This is an effect of the scale size used. In order to display the high transport values, the scale must be large compared to the relative
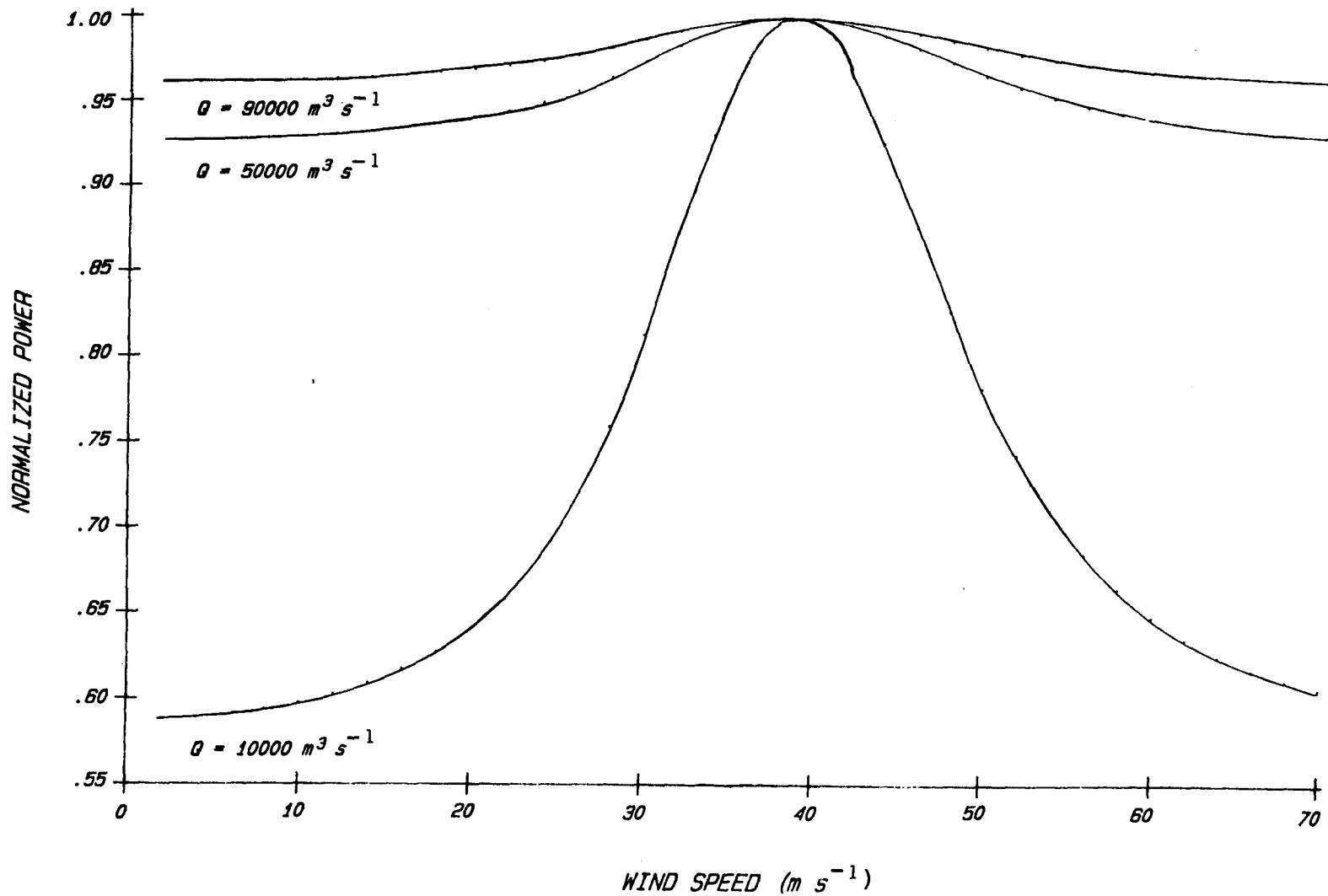
Figure 19 – Alongshore baroclinic power for various values of discharge, as a function of wind speed. Each curve is normalized to its maximum value.
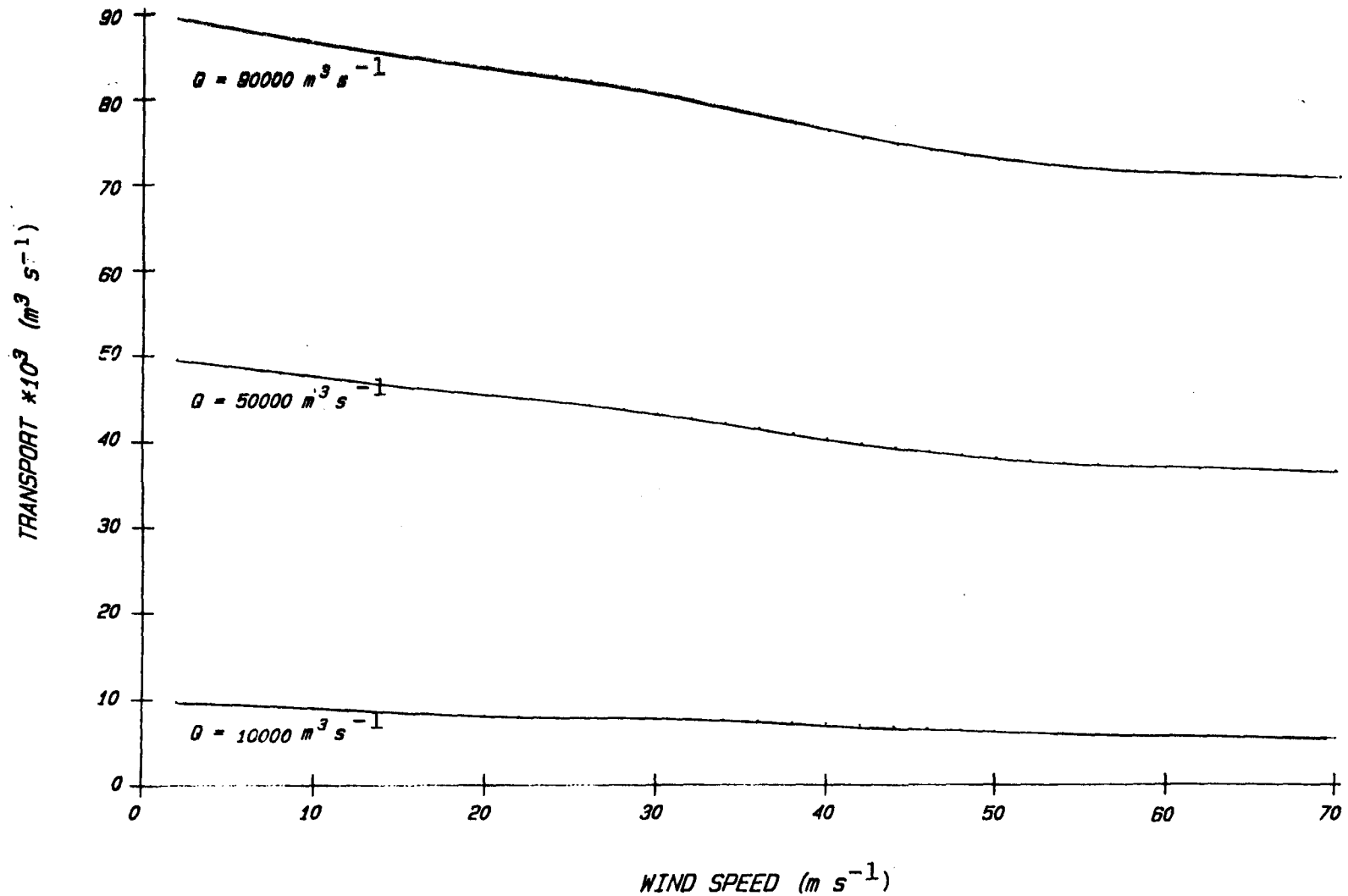
Figure 20 – Alongshore fresh water transport as a function of wind speed for various values of discharge.
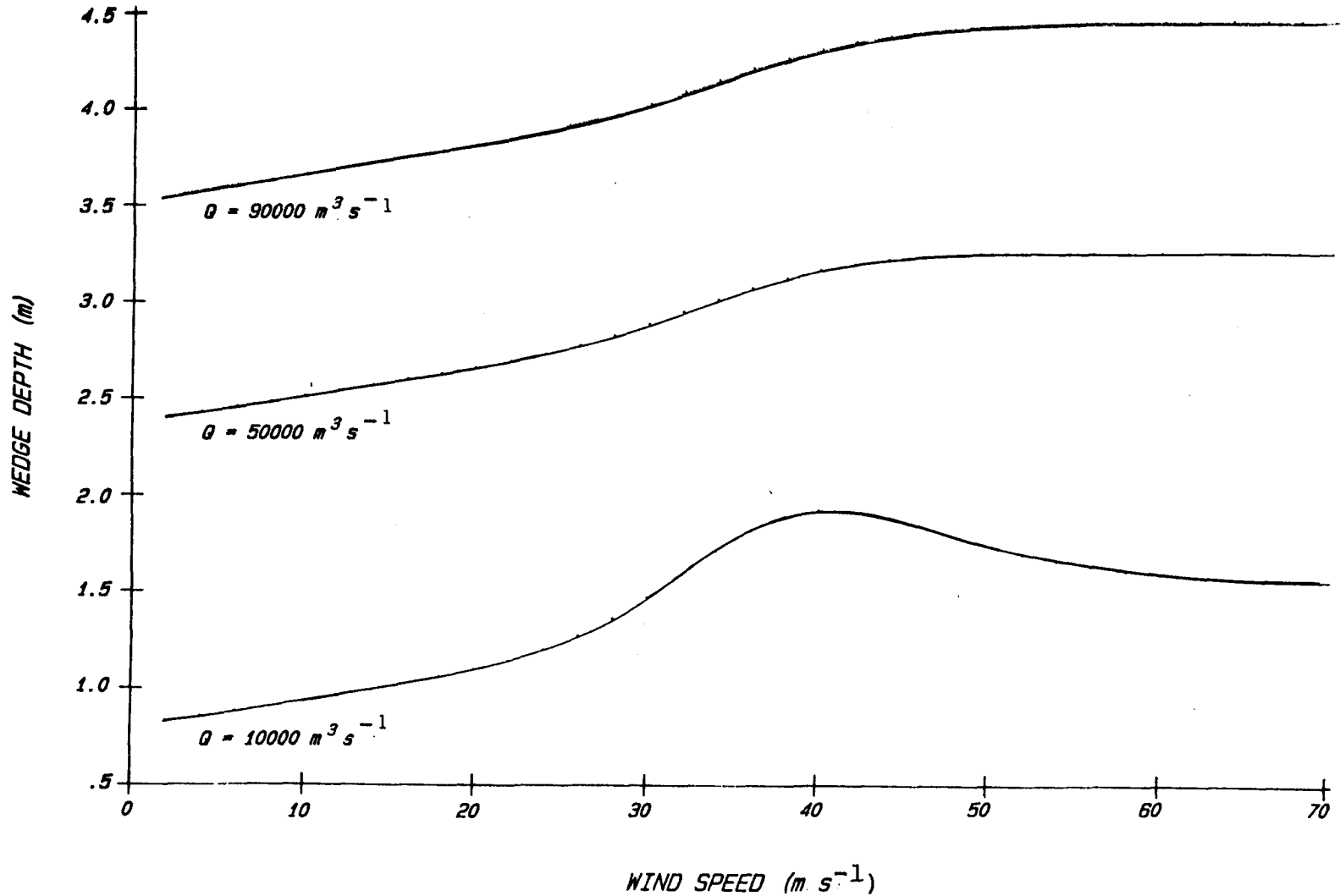
Figure 21 – Fresh water wedge depth at the coast as a function of wind speed for various values of discharge.
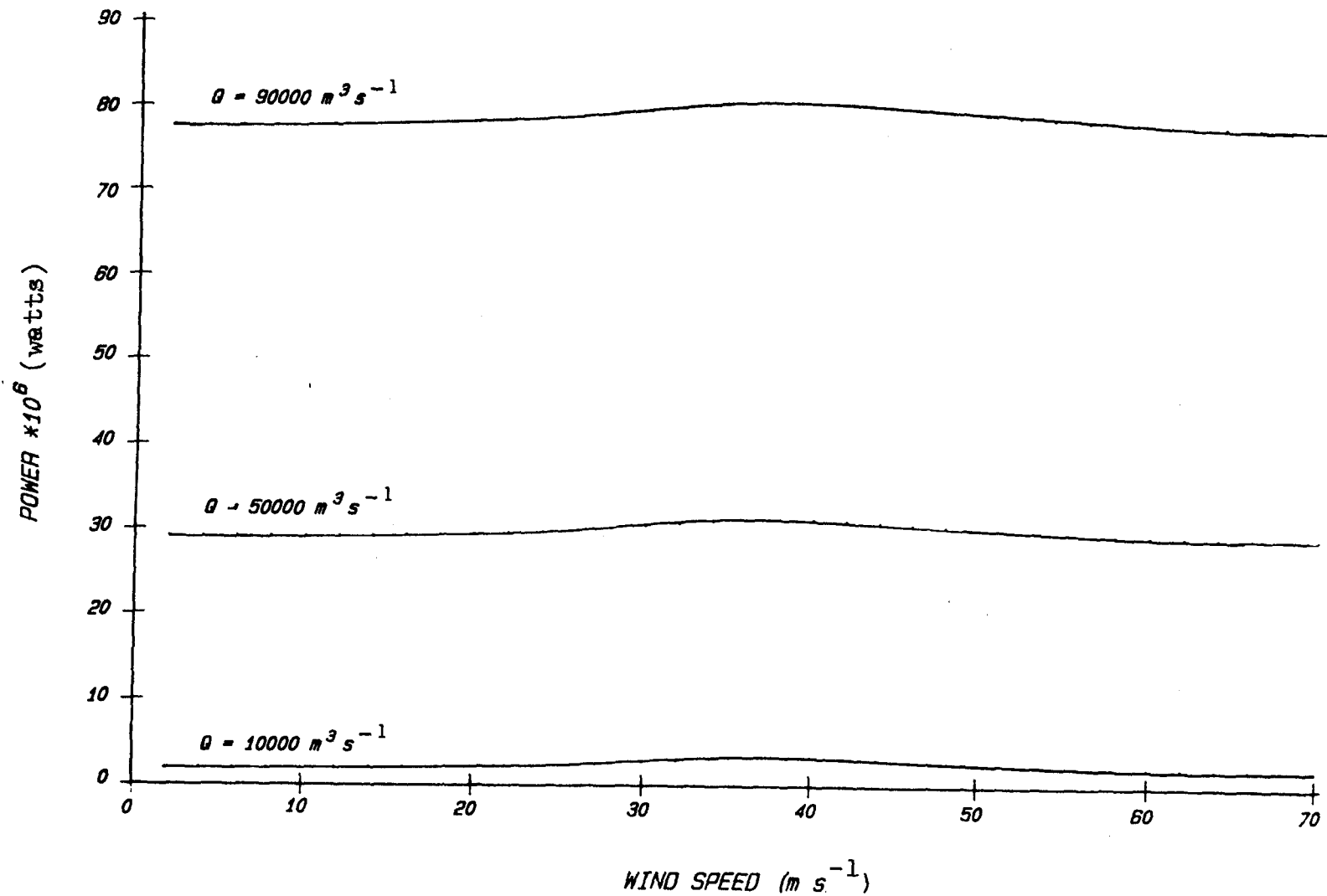
Figure 22 — Alongshore baroclinic power as a function of wind speed for various values of discharge.
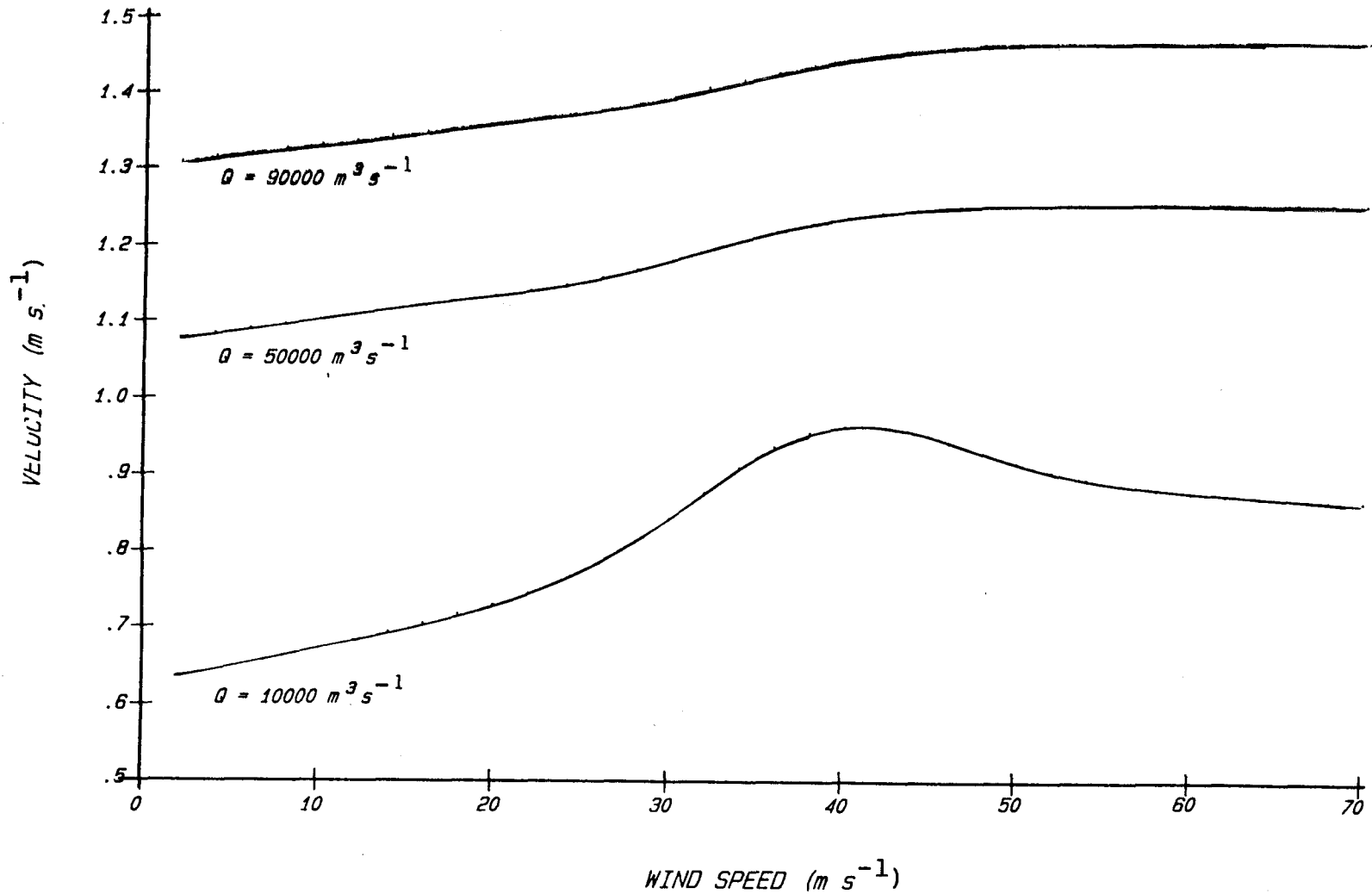
Figure 23 – Alongshore, baroclinic velocity of fresh water as a function of wind speed for various values of discharge.
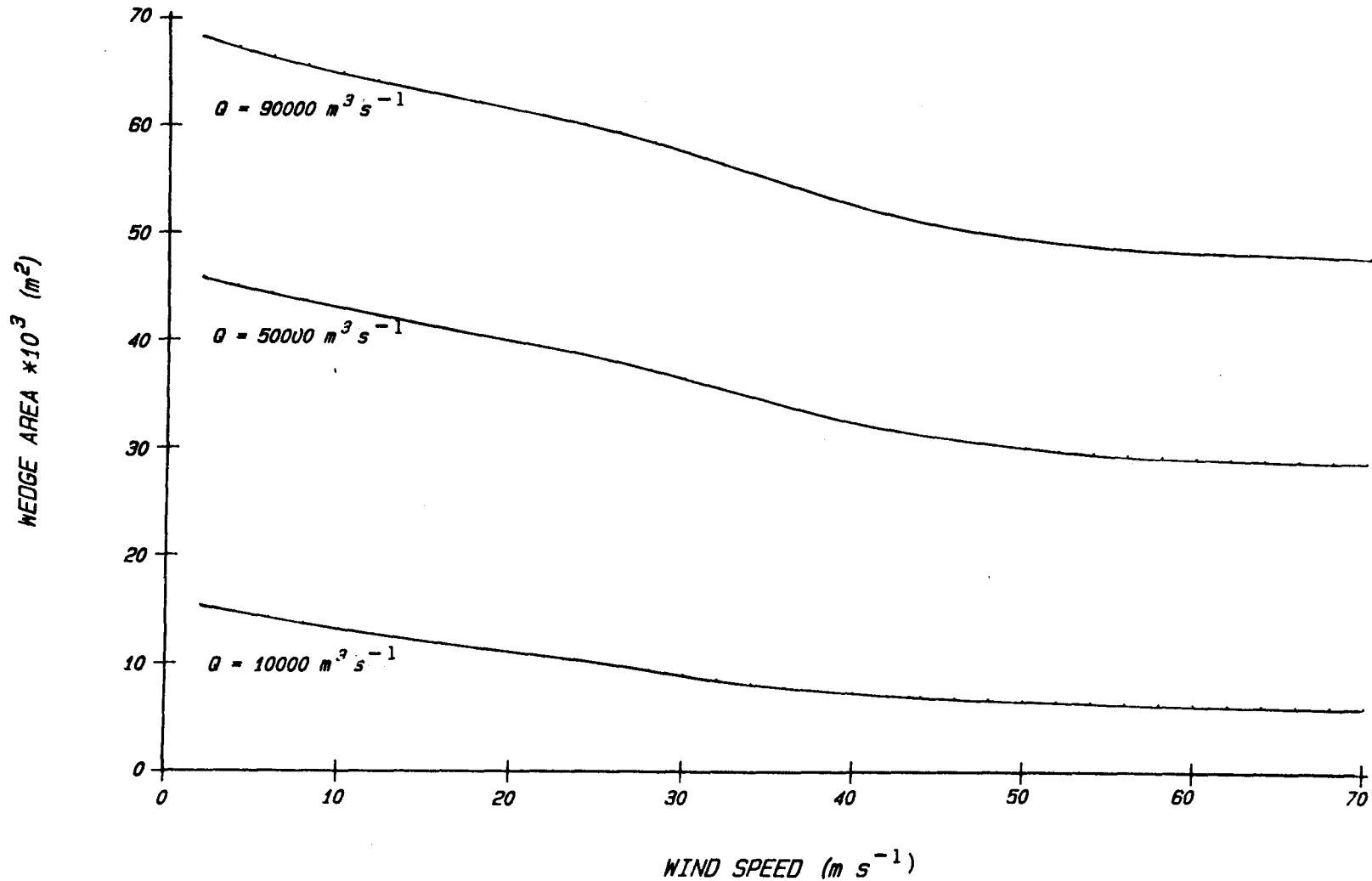
Figure 24 - Cross-sectional area of baroclinic fresh water wedge as a function
of wind speed for various values of discharge.
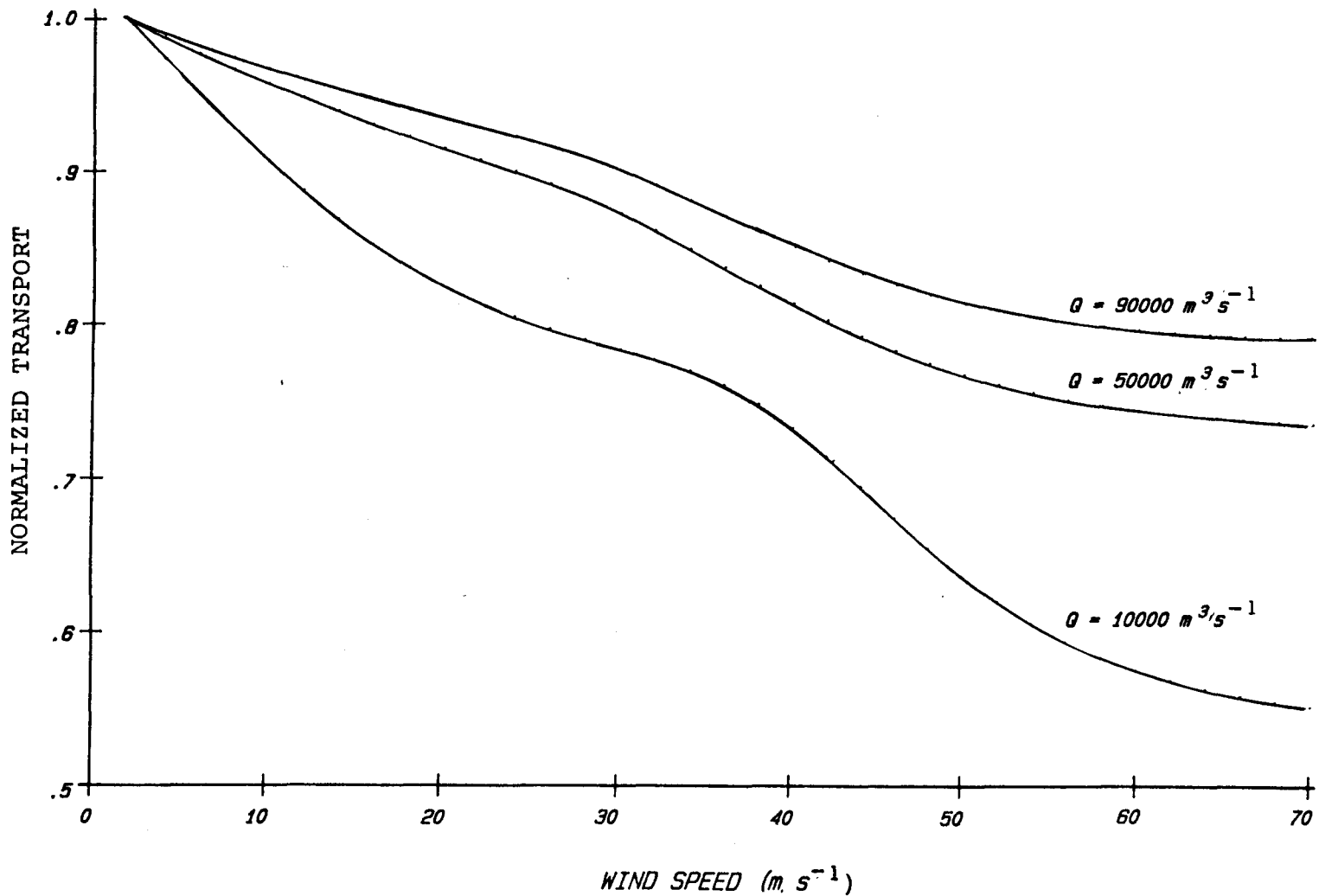
Figure 25 – Alongshore transport of fresh water as a function of wind speed for various values of discharge. Each curve is normalized to its value for W = 2 m s^{-1}.

alongshore wind speed of 6 m s^{-1}. Using these values in the model yields an average transit time of 35 days.

Royer (1981) did a statistical correlation for the wind speed, fresh water discharge, and alongshore transport. He found that by dividing the discharge area into two sections, Southcoast and Southeast Alaska (Figure 1), and lagging the two discharges by some period of time caused variation in the correlation coefficient. The lagging process allows the water from the southeastern coast sufficient time to arrive at the southern coast. Since the discharge values are based on a monthly mean, the time lagging was done for whole monthly values (0, 1, 2, 3). The best correlation was achieved for a lag time of one month, which is in good agreement with the value (35 days) predicted by the model.

By integrating over the depth of the fresh water layer, the vertical structure has been removed from the wind drift components. One way to incorporate vertical variations in such a problem is to adopt the approach used by Heaps (1980). Vertical variations of the baroclinic currents were included for his two-layer, baroclinically driven coastal current. The disadvantage of the Heaps model is the lack of wind forcing. If the best aspects of the two models were combined, the result would be a model with both vertical resolution and wind forcing.

The addition of time dependence would be a logical step toward a more complete predictive tool. This is evidenced by the highly variable wind intensities experienced along the southern coast of Alaska. A time scale on the order of a day or more (Neumann and Pierson, p. 207, 1966) is required to have fully developed wind drift currents. However, the wind varies greatly in intensity on an hourly basis. Therefore, there

is not sufficient time to have steady-state wind drift currents. The variability of the fresh water discharge has been determined on a monthly time scale. Due to the large drainage area and length of travel time there will be some smoothing of the discharge signal, decreasing its temporal fluctuations.

An indication of the relative temporal contributions due to wind and fresh water can be estimated by examining variations of these parameters. The mean monthly discharge values can vary by about 12000 m^3 s^{-1} from one month to the next. From the dischargees determined by Royer (1982), it may take 30 days for these changes to occur. The wind speed may vary from 5 m s^{-1} to 20 m s^{-1}, taking about a day for the effects to be fully realized. Applying these values to the model yields the values of temporal acceleration found in table I. The values indicate that the temporal accelerations of the current due to changes in wind speed are about 14 times greater than those due to changes in discharge. Therefore, the temporal variation of the wind will have a more profound effect on the current than the temporal variations of the fresh water discharge on relatively short time scales.

The baroclinic transport that has been dealt within this model is the component due to fresh water. In the actual current, the mixing process causes the resultant transport to consist of the fresh water and ambient baroclinic transport. Mork (1981) determined that, due to entrainment, about 2% of the total transport is due to fresh water. Applying average values of discharge, 23000 m^3 s^{-1}, and wind speed, 6 m s^{-1}, the transport predicted by the model is 21294 m^3 s^{-1}. If this is adjusted by Mork's 2% factor, the total transport is 1,096,000 m^3 s^{-1}. This value of transport is in good agreement with direct observations (Royer, 1981).

TABLE I − Temporal accelerations for changes in fresh water discharge and wind speed.

Varied wind speed for constant discharge

$\Delta t = 1$ day

$Q(m^3 s^{-1})$	$W(m\ s^{-1})$	$V_{bc}(m\ s^{-1})$	$\Delta V_{bc}(m\ s^{-1})$	$\Delta V_{bc}/t(m\ s^{-2})$	$\Delta V_{bc}/t(m\ s^{-2})$
23000	5	0.8456			
			0.0599	$6.9329\ 10^{-7}$	
23000	20	0.9055			
					$6.4930\ 10^{-7}$
35000	5	0.9686			
			0.0523	$6.0532\ 10^{-7}$	
35000	20	1.0209			

Varied discharge for constant wind speed

$\Delta t = 30$ days

23000	5	0.8456			
			0.1230	$0.4745\ 10^{-7}$	
35000	5	0.9686			
					$0.4599\ 10^{-7}$
23000	20	0.9055			
			0.1154	$0.4452\ 10^{-7}$	
35000	20	1.0209			

ASSUMPTIONS

It is prudent to address the degree to which the assumptions limit the model. As was mentioned earlier, the assumption of no mixing is inconsequential in the absence of wind, since mixing does not occur on a large scale. There will be some turbulent mixing due to the current motion itself. However, the energy produced from the resultant mixed system has been extracted from the current flow and there is no net change in the energy of the system. When wind is applied, the real coastal current, as opposed to the model, experiences mixing of fresh and sea water to some depth. Constraining the model to no mixing may seem to be a most stringent assumption. For our purposes, the main difference between a mixed and unmixed system is the level of potential energy. Equation (4) describes the potential energy as a function of fluid density and mixing depth. The potential energy described here consists of the energy from the unmixed system and the energy from mixing. The energy of mixing is provided by the wind, which is accounted for in the model by including the power supplied by the wind, P_w. The power, P_o, of the unmixed system and P_w yield the total power, P_{bc}, expected from the baroclinic process. By using the power balance, a mixed system has been well represented by a model that assumes no mixing.

Due to the steady-state nature of the model, it is limited to making long term (monthly) predictions of the behavior of the coastal current. Although the relative importance of the wind and discharge effects can be assessed, short term (hourly or daily) variations are not possible.

Royer (1982) has shown that the runoff pattern for the fresh water flowing into the ocean can be well approximated by a line source. Therefore, the line source assumption should be of no limiting consequence to the model.

52

The mean monthly wind field has been shown (Livingstone and Royer [1980]) to have a fairly steady westerly trend. Storm surges can not be considered due to their transient nature. Thus, the model is limited by its steady-state nature.

A straight, finite coast and constant shelf depth mainly eliminate localized distortions of the velocity fields, but have no effect on transport and average velocity of the current. Also, the Coriolis parameter varies little over the geographical region covered by the current and should not affect the average properties of the current.

Horizontal friction is negligible since the width of the current is large compared to the distance that friction effects are experienced in relation to the coast.

Chapter IV   SUMMARY

An analytical model has been developed to explore a possible mechanism by which an easterly, alongshore wind and coastal fresh water discharge interact to produce a westward flowing coastal current. The coastal current borders the southern and southeastern coasts of Alaska. The steady-state, two-layer model has two fundamental tenets: 1) the total alongshore transport of fresh water must equal the total influx of fresh water from the 1300 km coastline, ignoring the influx from the upper end, and 2) the alongshore baroclinic power must be the sum of the alongshore baroclinic power without wind and the power from the cross-shelf wind-induced drift currents. An analogy can be made between the baroclinic pressure gradient induced across the interface of the two layers and the voltage gradient in an electrical capacitor. Thus, the current is modeled as a fluid capacitor.

The average coastal transit time and total transport values predicted by the model are in good agreement with direct observations. Wind has been shown to have a significant effect on the current. Using this steady-state model, it is estimated that wind variations will have greater temporal effects, on the current, than variations in discharge.

Future modelling efforts should concentrate on: 1) incorporating vertical resolution for both the wind drift and baroclinic currents and 2) developing a transient scheme sensitive to short term (hourly) variations. The ultimate goal of the modelling efforts is to develop a reliable tool for predicting the behavior of the coastal current using the coastal rainfall and wind conditions.

REFERENCES

Csanady, G. T., (1976)
    Mean Circulation in Shallow Seas. J. Geophys. Res., 81, 5389-5399.

Ekman, V. W., (1905)
    On the influence of the earth's rotation of ocean currents.
    Ark. f. Mat., Astron. och Fysik, 2, 1-53.

Griffiths, R. W., and P. F. Linden, (1980)
    THE STABILITY OF BOUYANCY-DRIVEN COASTAL CURRENTS. Dynamics of
    Atmospheres and Oceans, 5, 281-306.

Haakstad, M., (1977)
    The lateral movement of the coastal water and its relation to
    vertical diffusion. Tellus, 29, 144-150.

Heaps, N. S., (1972)
    Estimation of Density Currents in the Liverpool Bay Area of the
    Irish Sea. Geophys. J.R. astr. Soc., 30, 415-432.

Heaps, N. S., (1980)
    Density currents in a two-layered coastal system, with application
    to the Norwegian Coastal Current. Geophys. J. R. astr. Soc., 63,
    289-310.

Kao, T. W., (1981)
    The Dynamics of Ocean Fronts. Part II: Shelf Water Structure
    Due to Freshwater Discharge. J. Phys. Oceanogr., 11, 1215-1223.

Leetma, A., (1976)
    Marine Sediment Transport and Environmental Management. Edited by
    D. J. Stanley and D. J. P. Swift, New York, N. Y.: John Wiley &
    Sons Inc.

Livingstone, D., and T. C. Royer, (1980)
    Observed Surface Winds at Middleton Island, Gulf of Alaska and
    Their Influence on the Ocean Circulation. J. Phys. Oceanogr., 10,
    753-764.

Mork, M., (1981)
    EXPERIMENTS WITH THEORETICAL MODELS OF THE NORWEGIAN COASTAL CUR-
    RENT. Proceedings from the Norwegian Coastal Current Symposium,
    Geilo, Volume II, University of Bergen Press, 518-530.

Neumann, G., and W. J. Pierson Jr., (1966)
    PRINCIPLES OF PHYSICAL OCEANOGRAPHY. Englewood Cliffs, N. J.:
    Prentice-Hall, Inc., 545 pp.

Pedlosky, J., (1979)
    Geophysical Fluid Dynamics. New York, N. Y.: Springer-Verlag,
    624 pp.

Pietrafesa, L. J., and G. S. Janowitz, (1979)
    On the effects of Bouyancy Flux on Continental Shelf Circulation.
    J. Phys. Oceanogr., 9, 911-918.

Pond, S., and G. L. Pickard, (1978)
    INTRODUCTORY PHYSICAL OCEANOGRAPHY. New York, N. Y.: Pergamon
    Press, 241 pp.

Royer, T. C., (1981)
    Baroclinic transport in the Gulf of Alaska Part II. A fresh water
    driven coastal current. Journal of Marine Research, Volume 39, 2,
    251-266.

Royer, T. C., (1982)
    Coastal Fresh Water Discharge in the Northeast Pacific.
    J. Geophys. Res., 87, 2017-2021.

Shearer, J. L., A. T. Murphy, and H. H. Richardson, (1967)
    INTRODUCTION TO SYSTEMS DYNAMICS. Reading, MA.: Addison-Wesley,
    420 pp.

Stommel, H., and A. Leetma, (1972)
    Circulation on the Continental Shelf. Proc. Nat. Acad. Sci. USA,
    69, 3380-3384.

APPENDIX A

Derivation of sea surface wedge area, A_t.

N - seaward sea slope extent (m)

η - sea height at coast (m)

ψ - sea height at distance (M-S) from coast (m)

$$\tan(\beta) = \eta/N \quad (1a)$$

$$\tan(\beta) = \psi/(N+S-M) \quad (2a)$$

$$\text{total area} = N\,\eta/2 \quad (3a)$$

$$\text{partial area} = \psi(N+S-M) \quad (4a)$$

$$A_t = N\,\eta/2 - \psi(N+S-M)/2 \quad (5a)$$

Solving equations (1a) for η, (2a) for ψ, and substituting into equation (5a) yields:

$$A_t = N^2 \tan(\beta)/2 - (N+S-M)^2 \tan(\beta)/2 \quad (6a)$$

$$A_t = \tan(\beta)/2 \, (N^2 - (N-M+S)^2) \quad (7a)$$

Equation (7a) is the form found in the main text.

APPENDIX B

List of equations describing P_w.

$P_w = \rho_a/64/C$ (1/3 (L/3/C/h (T1 sinh3J cos3J-T1 sinh3E cos3E-T2 cosh3J sin3J+T2 cosh3E sin3E)-L (ST1 sinh3E sin3E+cosh3E cos3E))+1/5 (3 L/5/C/h (T3 sinh3J cosJ-T3 sinh3E cosE-T4 cos3J sinJ+T4 cosh3E sinE+T5 sinhJ cos3J-T5 sinhE cos3E-T6 coshJ sin3J+T6 coshE sin3E)-L (ST3 sinh3E sinE+ST4 cosh3E cosE+ST5 sinhE sin3E+ST6 coshE cos3E))+3 L/C/h (T7 sinhJ cosJ-T7 sinhE cosE-T8 coshJ sinJ+T8 coshE sinE)-L (ST7 sinhE sinE+ST8 coshE cosE))

$$AL3 = \alpha^3$$

$$GA3 = \gamma^3$$

$$ASG = \alpha^2 \gamma$$

$$GSA = \gamma^2 \alpha$$

ST1 = -AL3+3 ASG+3 GSA-GA3   T1 = 3 ASG-GA3

ST2 = -AL3-3 ASG+3 GSA+GA3   T2 = -AL3+3 GSA

ST3 = -3 AL3+9 ASG-3 GSA+9 GA3   T3 = +4 AL3+3 ASG+4 GSA+3 GA3

ST4 = -9 AL3-3 ASG-9 GSA-3 GA3   T4 = -3 AL3+4 ASG-3 GSA+4 GA3

ST5 = +9 AL3-3 ASG+9 GSA-3 GA3   T5 = +4 AL3-3 ASG+4 GSA-3 GA3

ST6 = +3 AL3+9 ASG+3 GSA+9 GA3   T6 = +3 AL3+4 ASG+3 GSA+4 GA3

ST7 = +9 AL3-3 ASG-3 GSA+9 GA3   T7 = -ASG+3 GA3

ST8 = +9 AL3+3 ASG-3 GSA-9 GA3   T8 = 3 AL3-GSA